14 August 2020

The yeast ISW1b ATP-dependent chromatin remodeler is critical for nucleosome spacing and dinucleosome resolution

Peter R. Eriksson and David J. Clark [1]

Division of Developmental Biology, *Eunice Kennedy Shriver* National Institute of Child Health and Human Development, National Institutes of Health, Bethesda, Maryland 20892, USA

[1] **For correspondence:** clarkda@mail.nih.gov. Tel. 301 496-6966.
Building 6A Room 2A02, 6 Center Drive, Bethesda MD 20892.

Competing interests: The authors declare that no competing interests exist.

Abstract

Isw1 and Chd1 are ATP-dependent nucleosome-spacing enzymes required to establish regular arrays of phased nucleosomes near transcription start sites of yeast genes. Cells lacking both Isw1 and Chd1 have extremely disrupted chromatin, with weak phasing, irregular spacing and a propensity to form closed-packed dinucleosomes. The Isw1 ATPase subunit occurs in two different remodeling complexes: ISW1a (composed of Isw1 and Ioc3) and ISW1b (Isw1, Ioc2 and Ioc4). We show that ISW1b is primarily responsible for setting nucleosome spacing and resolving some close-packed dinucleosomes, whereas ISW1a plays only a minor role. Chd1 also separates some dinucleosomes, but not all. Dinucleosome accumulation correlates with RNA polymerase II levels, except for very highly transcribed genes, which are partially depleted of dinucleosomes and mononucleosomes. Loss of the Set2 H3-K36 methyltransferase partly phenocopies loss of Ioc4, whereas loss of the Set1 H3-K4 methyltransferase has no global effect. In conclusion, ISW1b is critical for yeast chromatin organization.

Introduction

Eukaryotic DNA is packaged into the nucleus in the form of chromatin. The structural subunit of chromatin is the nucleosome, which is composed of an octamer of core histones (two molecules each of H3, H4, H2A and H2B), around which is wrapped ~146 bp of DNA in ~1.7 superhelical turns (***Luger et al., 1997***). Nucleosomes are regularly spaced along the DNA, like beads on a string, forming a fibre which spontaneously folds into higher-order chromatin structures (***Thoma et al., 1979***). Nucleosomes restrict access to DNA and are potent inhibitors of transcription and other DNA-dependent processes in vitro. Cells regulate access to their DNA in part by deploying ATP-dependent chromatin remodeling complexes that are capable of overcoming the nucleosome, either by removing it from the DNA or by sliding it along the DNA ***(Chereji and Clark, 2018; Clapier et al., 2017; Paul and Bartholomew, 2018; Prajapati et al., 2020***).

The ISWI and CHD enzymes represent a major class of ATP-dependent chromatin remodelers conserved from yeast to mammals. They are primarily nucleosome sliding enzymes; many have nucleosome spacing activity in vitro (***Ito et al., 1997; Lieleg et al., 2015; Lusser et al., 2005; Pointner et al., 2012; Stockdale et al., 2006; Torigoe et al., 2013; Tsukiyama et al., 1999***). In vivo, ISWI enzymes are important for chromatin organization near promoters and other gene regulatory elements in vivo (***Barisic et al., 2019; Gkikopoulos et al., 2011; Ocampo et al., 2016; Wiechens et al., 2016***). ISWI complexes have additional functions in chromatin assembly (***Ito et al., 1997; Lusser et al., 2005; Vary et al., 2004***), stress-induced gene repression (***Lindstrom et al., 2006; Pinskaya et al., 2009***), transcript termination (***Morillon et al., 2003; Ocampo et al., 2019***) and quality control of mRNP biogenesis (***Babour et al., 2016***).

The budding yeast (*Saccharomyces cerevisiae*) possesses at least four ATP-dependent chromatin remodeling complexes capable of spacing nucleosomes in vitro: ISW1, ISW2, Chd1 and INO80 (***Krietenstein et al., 2016; Tsukiyama et al., 1999; Udugama et al., 2011; Vary et al., 2003***). In vivo, global chromatin organization in cells lacking Isw2 is very similar to wild type (***Gkikopoulos et al., 2011; Ocampo et al., 2016***), suggesting that ISW2 activity is more local than global. In contrast, cells lacking Ino80 (***Qiu et al., 2020; van Bakel et al., 2013; Yen et al., 2012***) or Isw1 (***Ocampo et al., 2016; Tirosh et al., 2010***) have shorter average nucleosome spacing than wild type cells. Cells lacking Chd1 have slightly shorter spacing and relatively poor nucleosome phasing (***Gkikopoulos et al., 2011; Ocampo et al., 2016***). Most impressively, cells lacking both Isw1 and Chd1 have extremely disrupted chromatin, indicating that both enzymes are required for proper chromatin organization (***Gkikopoulos et al., 2011; Ocampo et al., 2016***). Recently, we showed that an important contributory factor to chromatin disruption in the *chd1Δ isw1Δ* double mutant is a tendency for nucleosomes at the 5'-ends of yeast genes to be packed close together, resulting in dinucleosomes with little or no linker DNA (***Ocampo et al., 2019***). This observation suggests that Isw1 and/or Chd1 are critical for resolving dinucleosomes.

The yeast Isw1 ATPase subunit is found in two different complexes, termed ISW1a (containing Isw1 and Ioc3) and ISW1b (containing Isw1, Ioc2 and Ioc4) (***Mellor and Morillon, 2004; Vary et al., 2003***). There is genetic evidence for antagonistic interactions between ISW1a and ISW1b, suggesting that ISW1a has a negative role in transcription that is suppressed by ISW1b (***Lafon et al., 2012***). The Ioc subunits appear to have regulatory functions, since the isolated Isw1 subunit is inactive in vitro (***Vary et***

73 ***al., 2003***), unless the AutoN inhibitory domain is mutated (***Yan et al., 2019***). The ISW1a complex is a
74 potent nucleosome spacing enzyme in vitro (***Gangaraju and Bartholomew, 2007; Richmond, 2012; Vary***
75 ***et al., 2003***) and its structure has been determined, suggesting a mechanism involving separation of two
76 nucleosomes using a protein ruler (***Yamada et al., 2011***). The ISW1b complex is a weaker nucleosome
77 spacing enzyme than ISW1a in vitro (***Vary et al., 2003***). The Ioc2 subunit of ISW1b contains a PHD finger
78 (***Smolle et al., 2012***), which may bind H3-K4me3, suggesting that Isw1 binding to chromatin is mediated
79 by H3-K4 trimethylation (***Santos-Rosa et al., 2003***). The Ioc4 subunit of ISW1b has a PWWP domain
80 which binds to H3-K36me3, a histone modification associated with active transcription (***Maltby et al.,***
81 ***2012; Smolle et al., 2012***). These observations suggest that H3-K4 and H3-K36 trimethylation may play a
82 critical role in ISW1b function.
83 Although ISW1a and ISW1b have been studied in depth in vitro, relatively little is known about
84 their contributions to ISW1 function in vivo. Here, we have assessed the contributions of ISW1a and
85 ISW1b to nucleosome spacing and separation of dinucleosomes. We find that ISW1b is the major
86 spacing enzyme, whereas ISW1a plays a very minor role in global genic chromatin organization that is
87 revealed only in the absence of ISW1b. ISW1b, together with Chd1, is required to resolve
88 dinucleosomes, whereas ISW1a makes little contribution.
89
90
91 ## Results
92
93 **The ISW1b complex is the major nucleosome spacing enzyme in yeast**
94 We have used MNase-seq to determine the chromatin organization at yeast genes. Briefly, this
95 technique involves micrococcal nuclease (MNase) digestion of the chromatin in purified nuclei to
96 predominantly mononucleosomes. Suitably digested DNA samples are then used to construct libraries
97 for paired-end sequencing. Alignment to the yeast genome indicates the location of each sequenced
98 nucleosome. The midpoint of each sequence is assumed to represent the midpoint of the nucleosome
99 (also called the dyad). An average plot for all 5770 yeast genes is obtained by aligning all genes on their
100 transcription start site (TSS) or on their major +1 nucleosome position, summing all of the nucleosome
101 dyads on every gene, and normalizing to the genomic average (set at 1). A typical plot for wild type cells
102 is shown in ***Figure 1A***. We define nucleosome spacing as the average distance between the dyad peaks
103 for the +1 to +5 nucleosomes (i.e. the first five nucleosomes on the average gene), measured by the
104 slope of the regression line. However, in some mutants, the phasing is so poor that the spacing cannot
105 be measured accurately (see below). The degree of phasing is indicated by the height of the nucleosome
106 peaks: higher peaks indicate more coincident dyads and therefore better nucleosome positioning.
107 We have shown previously (***Ocampo et al., 2016***) that cells lacking Isw1 have weaker
108 nucleosome phasing and reduced spacing relative to wild type cells (***Figure 1B***). However, *isw1Δ* cells
109 lack both the ISW1a and the ISW1b remodeling complexes. To assess the relative contributions of ISW1a
110 and ISW1b to phasing and spacing, we examined the chromatin organization in various *ioc* mutants.
111 Cells lacking the ISW1a complex (*ioc3Δ*) show a slight increase in spacing (replicates: 166, 167 bp) with
112 no change in phasing relative to wild type (165, 165 bp) (***Figure 1C***). In contrast, cells lacking an ISW1b
113 subunit (*ioc2Δ* or *ioc4Δ*) have intermediate nucleosome spacing (161-163 bp) (***Figure 1D, E***): less than in

wild type (165 bp), but not as low as in *isw1Δ* cells (159, 160 bp). The spacing differences are mostly small, but they are clear, because the nucleosome shift increases with the nucleosome number (compare biological replicate experiments; ***Figure 1***). Phasing is weaker in the *ioc2Δ* mutant (***Figure 1D***), but hardly affected in the *ioc4Δ* mutant (***Figure 1E***). Cells lacking both ISW1b ancillary subunits (the *ioc2Δ ioc4Δ* double mutant) have similar chromatin organization to the *ioc2Δ* single mutant, exhibiting the weaker phasing observed in *ioc2Δ* cells as well as the shorter spacing observed in both the *ioc2Δ* and *ioc4Δ* single mutants (***Figure 1F***). The similar spacing in the *ioc2Δ* and *ioc4Δ* single mutants and the *ioc2Δ ioc4Δ* double mutant (~162 bp) suggests that both Ioc2 and Ioc4 are required for ISW1b spacing activity.

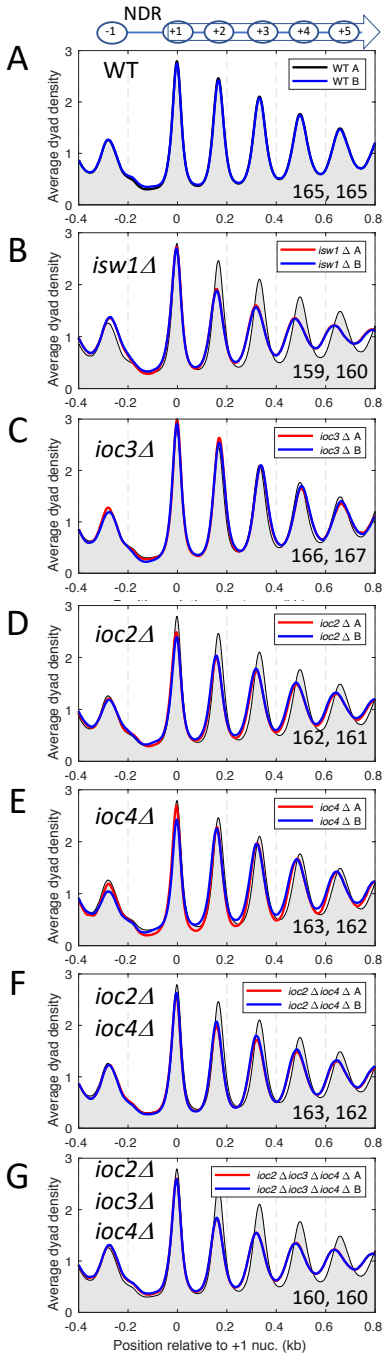

Figure 1. The ISW1b complex (Isw1-Ioc2-Ioc4) is required for setting wild type nucleosome spacing, whereas the ISW1a complex (Isw1-Ioc3) sets intermediate spacing in the absence of ISW1b. Average nucleosome dyad density plots for all genes: (**A**) wild type, (**B**) *isw1Δ*, (**C**) *ioc3Δ*, (**D**) *ioc2Δ*, (**E**) *ioc4Δ*, (**F**) *ioc2Δ ioc4Δ*, (**G**) *ioc2Δ ioc3Δ ioc4Δ*. All yeast genes were aligned on the midpoints of their +1 nucleosomes. The dyad distribution was normalized to the global average (set at 1). For ease of comparison, wild type (WT) replicate A is shown as a black line with grey fill in all plots. Two biological replicate experiments (A and B) are shown for each strain in all of the plots (A: red line; B: blue line). The average spacing in bp is shown for replicates A and B in the bottom right corner (measured by regression analysis of the first 5 nucleosome peaks, beginning with the +1 nucleosome).

123 Chromatin organization in cells lacking all three ancillary subunits (the *ioc2Δ ioc3Δ ioc4Δ* triple
124 mutant) is very similar to that in *isw1Δ* cells (***Figure 1G***). This is expected, because both complexes
125 should be inactive in both mutants, given that the Isw1 subunit by itself has no remodeling activity in
126 vitro (***Vary et al., 2003***), but it also implies that ISW1a affects spacing since the triple mutant is not the
127 same as the *ioc2Δ ioc4Δ* double mutant. The shorter spacing in the *ioc2Δ ioc3Δ ioc4Δ* triple mutant is
128 suggests that ISW1a is responsible for the intermediate spacing observed in the absence of ISW1b. Since
129 the loss of Ioc3 has only a small effect on global spacing in the presence of ISW1b (the *ioc3Δ* single
130 mutant), ISW1b is more important for chromatin organization than ISW1a. That is, the contribution of
131 ISW1a is only clear at the global level if ISW1b is absent. We conclude that the ISW1b complex is
132 primarily responsible for wild type nucleosome spacing and that the ISW1a complex has a minor
133 underlying role, mediating intermediate spacing.
134
135 **ISW1a and ISW1b activities are not restricted to target genes**
136 Chromatin immunoprecipitation (ChIP-seq) experiments have shown that ISW1a (Ioc3), ISW1b (Ioc4)
137 and Isw1 are enriched on different sets of genes (***Yen et al., 2012***). We determined whether the
138 chromatin organization of these sets of target genes is differentially affected by loss of ISW1a or ISW1b,
139 as might be expected. In the case of ISW1a, we found that Ioc3-target genes show very slightly increased
140 spacing (166 vs. 165 bp) in wild type cells and in *ioc3Δ* cells (167 vs. 166 bp), but these differences are
141 probably negligible (***Figure S1A***). Thus, ISW1a has little or no differential effect on the chromatin
142 organization of its target genes. Moreover, the spacing on Ioc3-bound genes is affected in *ioc4Δ* cells,
143 indicating that ISW1a target genes are affected by ISW1b (Ioc4) (***Figure S1A***). In the case of ISW1b, Ioc4-
144 target and non-target genes have the same spacing and phasing in wild type cells, suggesting that they
145 are not differentially affected by ISW1b. In *ioc4Δ* cells, both sets of genes have shorter spacing than wild
146 type (***Figure S1B***). Ioc4-target genes may have slightly shorter spacing than non-target genes, but the
147 effect is subtle (***Figure S1B***). As expected, Ioc4-bound genes are not affected in *ioc3Δ* cells (***Figure S1B***).
148 Thus, ISW1b affects the chromatin organization of both target genes and non-target genes. Finally, Isw1-
149 target genes have the same spacing as non-target genes in wild type cells and, although the phasing is
150 slightly better on the Isw1-target genes, this effect is also observed in the absence of Isw1 (***Figure S1C***).
151 Isw1-target and non-target genes show similar changes in *isw1Δ* cells (short spacing and weaker
152 phasing), although there is a slight difference in spacing of 1-2 bp between target and non-target genes
153 (***Figure S1C***). Overall, the Isw1 complexes affect the chromatin organization of both target and non-
154 target genes similarly, with only subtle differences at most. It is unclear why we do not observe obvious
155 differences in chromatin organization for target and non-target genes defined by Ioc3, Ioc4 or Isw1
156 binding; perhaps all genes have some bound ISW1b, such that designated target genes are only
157 modestly enriched relative to non-target genes.
158
159 **ISW1b and Chd1 account for the extreme chromatin disruption in cells lacking both Isw1 and Chd1**
160 Cells lacking Chd1 have a mild chromatin organization defect (***Gkikopoulos et al., 2011; Ocampo et al.,***
161 ***2016***), characterized by somewhat shorter spacing than wild type (164, 163 bp vs. 165, 165 bp) and
162 weaker phasing (***Figure 2A***). In contrast, cells lacking both Chd1 and Isw1 (the *chd1Δ isw1Δ* double
163 mutant) have extremely disrupted chromatin organization (***Gkikopoulos et al., 2011; Ocampo et al.,***
164 ***2016***) (***Figure 2B***). We observed that the *chd1Δ ioc2Δ ioc4Δ* triple mutant (***Figure 2C***) also has extremely

disrupted chromatin, whereas the *chd1Δ ioc3Δ* double mutant is very similar to the *chd1Δ* single mutant (***Figure 2D***). This observation is consistent with our conclusion that the ISW1b complex is much more important than the ISW1a complex for global nucleosome spacing (***Figure 1***). However, chromatin organization in the *chd1Δ ioc2Δ ioc4Δ* triple mutant is not quite as severely disrupted as in the *chd1Δ isw1Δ* double mutant: the phasing in the triple mutant is very poor, but somewhat stronger than in the double mutant (***Figure 2B, C***). Measurement of the spacing in these two mutants is not appropriate because most of the peaks are too weak to measure accurately. The difference between the *chd1Δ ioc2Δ ioc4Δ* triple mutant and the *chd1Δ isw1Δ* double mutant is that the ISW1a complex (Isw1-Ioc3) is still present in the former mutant. This suggests that ISW1a contributes some residual order to genic chromatin in the absence of both Chd1 and ISW1b.

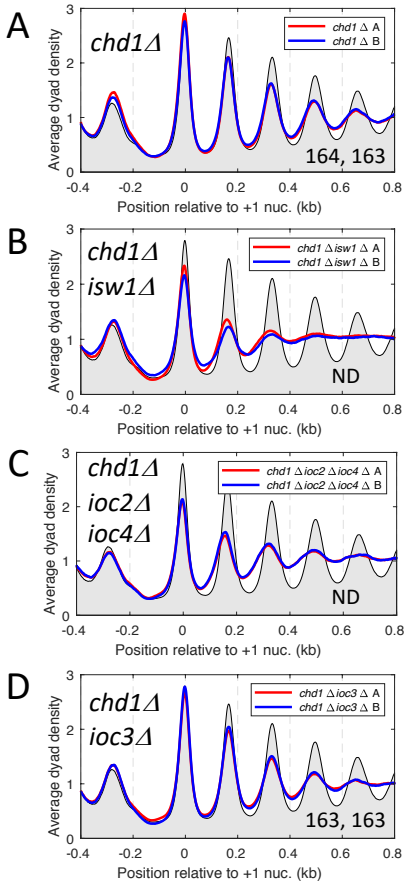

Figure 2. ISW1b and Chd1 are the major remodelers required for normal chromatin organization. Average nucleosome dyad density plots for all genes: (**A**) *chd1Δ*, (**B**) *chd1Δ isw1Δ*, (**C**) *chd1Δ ioc2Δ ioc4Δ*, (**D**) *chd1Δ ioc3Δ*. All yeast genes were aligned on the midpoints of their +1 nucleosomes. The dyad distribution was normalized to the global average (set at 1). For ease of comparison, wild type replicate A is shown as a black line with grey fill in all plots. Two biological replicate experiments (A and B) are shown for each strain in all of the plots (A: red line; B: blue line). The average spacing in bp is shown for replicates A and B in the bottom right corner (measured by regression analysis of the first 5 nucleosome peaks, beginning with the +1 nucleosome); ND = not determined because the phasing is too weak for accurate measurement.

ISW1a and ISW1b have little effect on the chromatin of very active genes

Since ISW1b associates with transcriptionally active genes (***Maltby et al., 2012***), we examined whether ISW1a or ISW1b mediate specific effects at highly active genes. We compared the average chromatin structure of the 300 most active genes, defined by ChIP-seq for the Rpb3 subunit of Pol II (***Ocampo et al., 2016***), with that of the remaining, less active, 5470 genes (***Figure S2***). In wild type cells, the chromatin of the highly active genes is poorly organized, characterized by much reduced and irregular spacing, weak phasing and a much wider nucleosome-depleted region (NDR) at the promoter, which extends upstream (***Cole et al., 2014; Weiner et al., 2010***). Although the average spacing on the highly active genes is difficult to measure accurately due to poor phasing, it is clearly shorter than the spacing

186 on the other genes (***Figure S2A***). The chromatin organization of the highly active genes is not strongly
187 differentially affected by any of the *ioc*Δ mutations or *isw1*Δ (***Figure S2A***), whereas the other genes have
188 the spacing observed for all genes, as expected. We conclude that ISW1a and ISW1b have no differential
189 effect on the chromatin organization of highly active genes, with the caveat that their general state of
190 disruption might obscure subtle effects. On the other hand, nucleosome phasing on the top 300 active
191 genes is weaker in cells lacking Chd1 than in wild type or in any of the *ioc* mutants (***Figure S2B***),
192 suggesting that Chd1 is the most important spacing enzyme for highly active genes, and consistent with
193 a direct association of Chd1 with transcript elongation factors (***Simic et al., 2003***).
194
195 **Both ISW1b and Chd1 are important for resolution of close-packed dinucleosomes**
196 We reported previously that a major contributing factor to chromatin disruption in the *chd1Δ isw1Δ*
197 double mutant is the presence of close-packed dinucleosomes, primarily involving the +2 nucleosome
198 (i.e. dinucleosomes containing either the +1 and +2 nucleosomes or the +2 and +3 nucleosomes)
199 (***Ocampo et al., 2019***) (***Figure 3A***). These dinucleosomes are characterized by MNase-resistant DNA
200 fragments of 250 - 350 bp, presumably representing two nucleosomes (or perhaps sub-nucleosomes)
201 with little or no intervening linker DNA for MNase to cut. The dyad plots shown above (***Figures 1 and 2***)
202 include only mononucleosome data because the analysis was limited to DNA fragments of 120 - 180 bp.
203 A dyad plot is not appropriate for dinucleosomes, since the midpoint of a dinucleosome would be
204 located between the two nucleosomes. Instead, we used nucleosome occupancy (coverage) plots, in
205 which the number of times each genomic base pair appears in either mononucleosomes or
206 dinucleosomes is counted and normalized to the genomic average. In the *chd1Δ isw1Δ* double mutant,
207 there is a strong dinucleosome peak at the +2 position and a depressed +2 mononucleosome peak,
208 consistent with the presence of a significant fraction of all +2 nucleosomes in dinucleosomes (Ocampo
209 et al., 2019) (***Figure 3A; Figure S3***). We determined the relative contributions of Chd1 and Isw1 to
210 dinucleosome resolution. A dinucleosome peak is observed in both the *chd1Δ* and *isw1Δ* single mutants,
211 but it is weaker than in the *chd1Δ isw1Δ* double mutant (***Figure 3A***). The +2 mononucleosome peak is
212 also weaker in the single mutants relative to wild type. These data indicate that the Chd1 and Isw1
213 remodeling enzymes both contribute independently and make additive contributions to dinucleosome
214 resolution, such that neither enzyme is capable of resolving all dinucleosomes on its own.
215 Next, we determined the separate contributions of the ISW1a and ISW1b complexes to Isw1-
216 dependent dinucleosome resolution (***Figure 3B***). The *ioc2Δ* and *ioc4Δ* single mutants have an enhanced
217 dinucleosome peak and depressed mononucleosome peak, as observed for the *isw1Δ* single mutant,
218 suggesting that both ancillary subunits of the ISW1b complex are required for Isw1-dependent
219 dinucleosome resolution. Consistent with this conclusion, the *ioc2Δ ioc4Δ* double mutant has a
220 dinucleosome peak similar to that in the single mutants. In contrast, there are fewer dinucleosomes in
221 the *ioc3Δ* mutant, which has a slightly lower +2 dinucleosome peak than wild type and somewhat higher
222 levels of the +2 and +3 mononucleosomes (***Figure 3B; Figure S3***), indicating that ISW1a is not important
223 for dinucleosome resolution. These conclusions are supported by high levels of dinucleosomes in the
224 *chd1Δ ioc2Δ ioc4Δ* triple mutant versus wild type, resulting from loss of both ISW1b and Chd1 (***Figure***
225 ***3C***). Similarly, the *chd1Δ ioc3Δ* double mutant has more dinucleosomes than wild type, but less than the
226 *chd1Δ ioc2Δ ioc4Δ* triple mutant, which can be accounted for by the absence of Chd1 with little

227 contribution from ISW1a (***Figure 3C***). Thus, the ISW1b complex accounts quite well for the role of Isw1
228 in dinucleosome resolution.
229

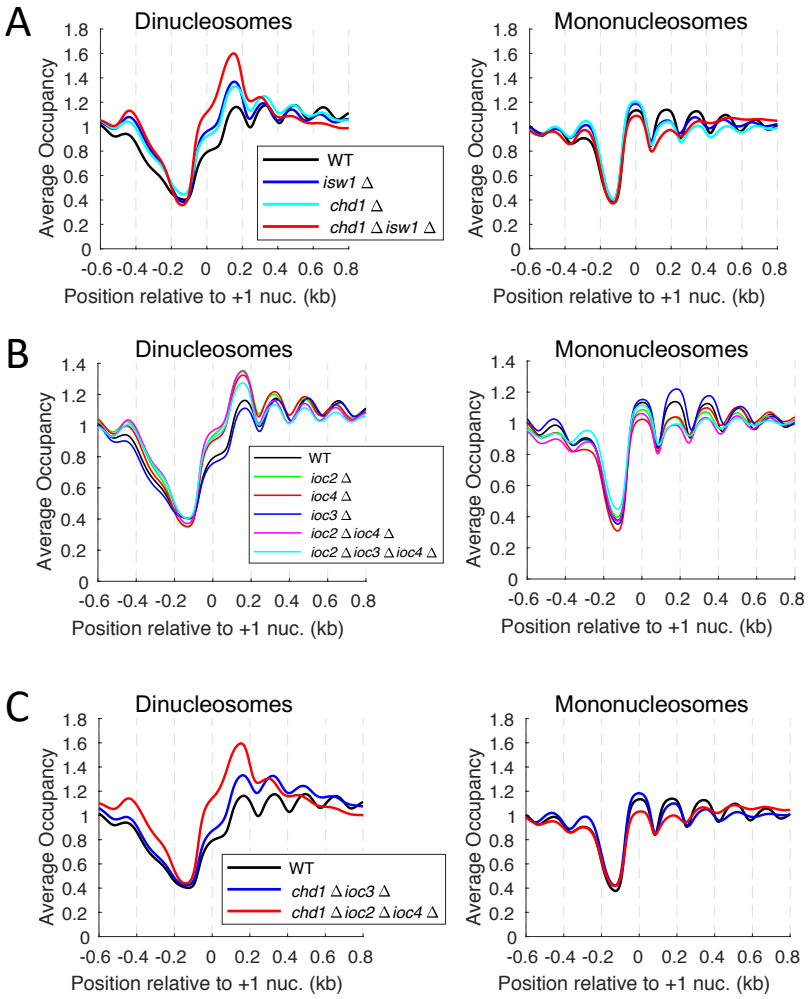

Figure 3. Both ISW1b and Chd1 are important for separating close-packed dinucleosomes. Average nucleosome occupancy (coverage) plots for all genes. All yeast genes were aligned on the midpoint of their average +1 nucleosome position. The occupancy was normalized to the global average (set at 1) for mononucleosomes (120 - 180 bp) or dinucleosomes (250 - 350 bp). Note different y-axis scales are used in different plots to separate the lines more clearly. Data for replicate A are shown (see ***Figure S3*** for comparison of biological replicate experiments). (**A)** Dinucleosomes involving the +2 nucleosome are enriched whereas +2 mononucleosomes are depleted in *chd1Δ isw1Δ* cells; smaller effects are observed in *chd1Δ* and *isw1Δ* cells. (**B)** ISW1b (Isw1-Ioc2-Ioc4) accounts for the increased level of dinucleosomes in *isw1Δ* cells. (**C)** ISW1b and Chd1 are both required to resolve all dinucleosomes.

230
231
232 **Dinucleosome formation correlates with RNA polymerase II levels**
233 Since highly active genes have much reduced nucleosome spacing (***Weiner et al., 2010***) (***Figure S2***), we
234 wondered whether transcription correlates with increased levels of dinucleosomes. We constructed
235 heat maps in which nucleosome occupancy data for all 5770 genes are aligned on the average +1
236 nucleosome position in wild type cells (set at 0 on the x-axis) and sorted by their Pol II density, as
237 measured by ChIP-seq for the Rpb3 subunit (Ocampo et al., 2016) (***Figure 4; Figure S4***). In wild type
238 cells, the +1 nucleosome is depleted in the dinucleosome heat map and well represented in the
239 mononucleosome heat map, indicating that there are relatively few +1/+2 dinucleosomes on all genes,
240 independent of Pol II level. However, in wild type cells, the prevalence of +2/+3 dinucleosomes does
241 correlate with gene activity, except for some of the top 300 highly active genes (***Figure 4A***; above the
242 horizontal dashed line). The latter are depleted of +2/+3 dinucleosomes, but somewhat enriched in
243 +4/+5 dinucleosomes instead, compared to other genes in the top 300 (***Figure 4A***). Mononucleosome
244 occupancy shows the opposite trend to dinucleosome occupancy: nucleosome occupancy on the 300

most active genes is relatively low, which we attribute to some loss of mononucleosomes to dinucleosome formation and to some nucleosome loss associated with transcription (***Cole et al., 2014; Cui et al., 2012; Schwabish and Struhl, 2007, 2004***). On all of the other genes, mononucleosome occupancy increases as Pol II density decreases, correlating with decreasing dinucleosome levels (***Figure 4A***; below dashed line). The least active genes, at the bottom of the heat map, clearly have fewer dinucleosomes and more mononucleosomes than the more active genes near the top of the heat map.

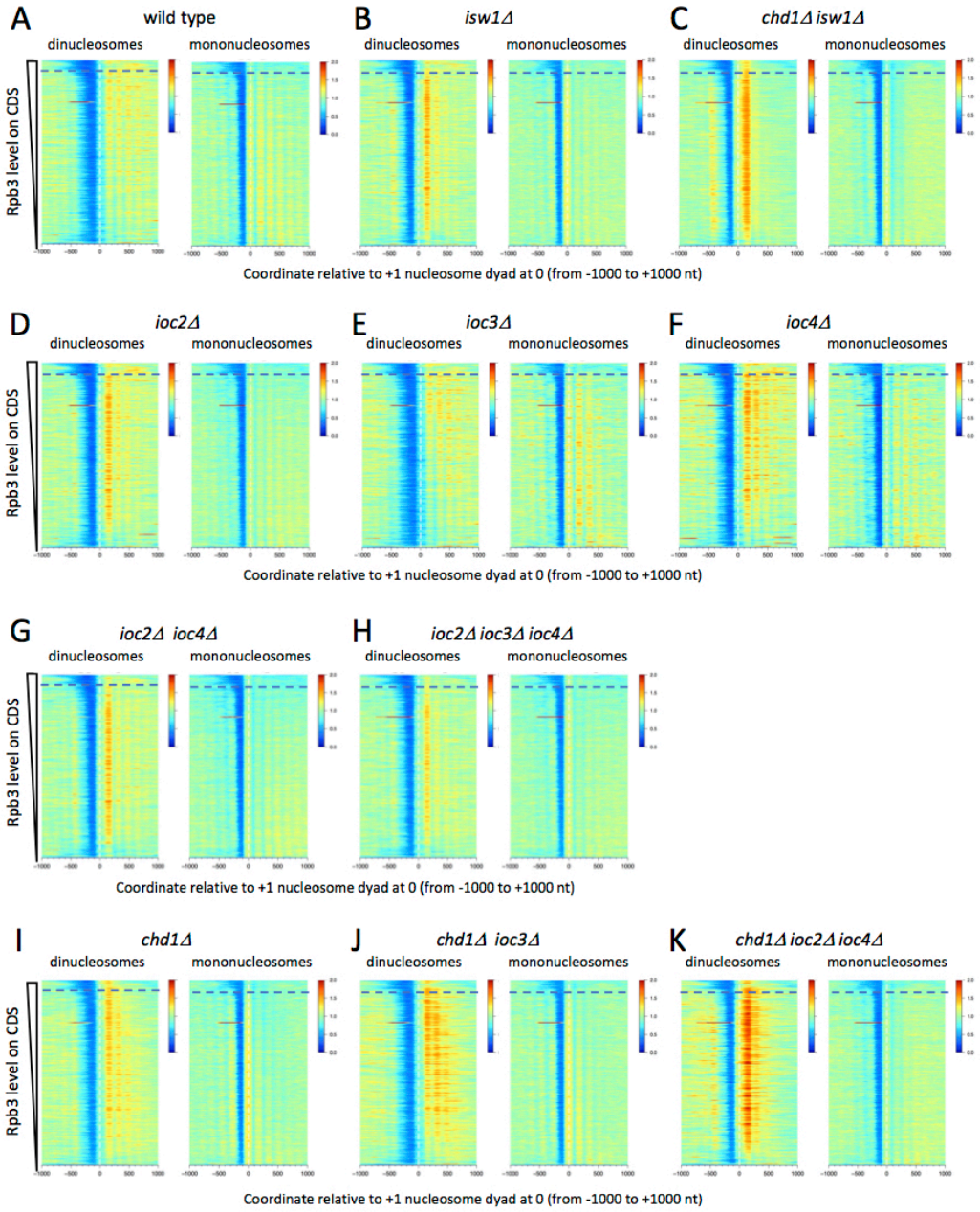

Figure 4. Dinucleosome formation correlates with RNA polymerase II levels, except for the most highly transcribed genes. Heat map analysis of nucleosome occupancy (coverage) for all 5770 genes aligned on the midpoint of their average +1 nucleosome position and sorted by Pol II density on the coding region (CDS), using ChIP-seq data for the Rpb3 subunit (***Ocampo et al., 2016***). Data for replicate A are shown (see ***Figure S4*** for replicate B). The dashed line separates the top 300 most active genes from the rest. The scale bar is the same for all plots, ranging from blue (low nucleosome occupancy) to red (high occupancy). (**A**) wild type, (**B**) *isw1Δ*, (**C**) *chd1Δ isw1Δ*, (**D**) *ioc2Δ*, (**E**) *ioc3Δ*, (**F**) *ioc4Δ*, (**G**) *ioc2Δ ioc4Δ*, (**H**) *ioc2Δ ioc3Δ ioc4Δ*, (**I**) *chd1Δ*, (**J**) *chd1Δ ioc3Δ*, (**K**) *chd1Δ ioc2Δ ioc4Δ*.

255 The trends observed in wild type cells are amplified in the *isw1Δ* single mutant (***Figure 4B***) and
256 very strongly amplified in the *chd1Δ isw1Δ* double mutant (***Figure 4C***); both have higher levels of
257 dinucleosomes than wild type (***Figure 3A***). In these two mutants, dinucleosomes involving the +2
258 nucleosome are much more prevalent relative to wild type, particularly in the bottom half of the heat
259 map where there is a greater increase in dinucleosomes relative to wild type; other dinucleosomes,
260 farther downstream, are much less prevalent relative to wild type (***Figure 4A-C***). In addition, in the
261 *chd1Δ isw1Δ* double mutant, the top 300 active genes are depleted of +4/+5 dinucleosomes. The least
262 active genes, right at the bottom of each heat map, remain low in dinucleosomes in both mutants
263 (***Figure 4A-C***).
264 The *ioc2Δ* single mutant, the *ioc2Δ ioc4Δ* double mutant and the *ioc2Δ ioc3Δ ioc4Δ* triple mutant
265 are all very similar to the *isw1Δ* mutant, whereas the *ioc4Δ* single mutant has higher levels of
266 downstream dinucleosomes than the other mutants and is more similar to wild type in this regard
267 (***Figure 4D-H***). In contrast, the *ioc3Δ* single mutant is similar to wild type (***Figure 4E***). This analysis
268 confirms that ISW1b is much more important than ISW1a for dinucleosome resolution. The *chd1Δ* single
269 mutant (***Figure 4I***) and the *chd1Δ ioc3Δ* double mutant (***Figure 4J***) are both quite similar to the *isw1Δ*
270 single mutant (***Figure 4B***). The *chd1Δ ioc2Δ ioc4Δ* triple mutant (***Figure 4K***) is very similar to the *chd1Δ*
271 *isw1Δ* double mutant (***Figure 4C***), again consistent with important roles for both Chd1 and ISW1b in
272 resolving dinucleosomes.
273 Overall, our data suggest that transcription is associated with higher levels of dinucleosomes,
274 perhaps formed by Pol II as it transcribes. The apparent anomaly of reduced dinucleosome prevalence
275 on the most active genes may be a consequence of transcription-associated nucleosome loss, which
276 strongly affects only the most active genes (***Cole et al., 2014; Schwabish and Struhl, 2007, 2004***).
277
278 **Loss of Set2 has a subtle effect on chromatin organization**
279 The Ioc4 PWWP domain binds preferentially to H3-K36me3 relative to unmethylated H3-K36 in vitro,
280 suggesting that ISW1b may be regulated by H3-K36me3 (***Maltby et al., 2012; Smolle et al., 2012***). The
281 only H3-K36 methyltransferase in yeast is encoded by *SET2*. Accordingly, we examined whether ISW1b-
282 mediated changes in nucleosome spacing and dinucleosome resolution depend on Set2 and H3-K36me3.
283 Nucleosome spacing in a *set2Δ* mutant (replicates: 165 and 163 bp) is slightly lower than wild type (165
284 and 165 bp), although this difference may not be significant (***Figure 5A***). Ioc4 has a clearer effect on
285 chromatin organization (***Figure 1E***; *ioc4Δ* replicates: 163 and 162 bp) than loss of Set2 (***Figure 5B***). Cells
286 lacking Set2 or Ioc4 show a similar correlation between dinucleosome levels and transcriptional activity
287 and show a somewhat higher prevalence of dinucleosomes than wild type (***Figure 5C and Figure S3***). We
288 conclude that loss of H3-K36me3 has some effect on ISW1b activity but does not fully nullify it, since
289 chromatin organization in the *set2Δ* mutant is not as defective as in the *ioc2Δ* or *ioc2Δ ioc4Δ* mutants
290 (***Figure 1D, F***).

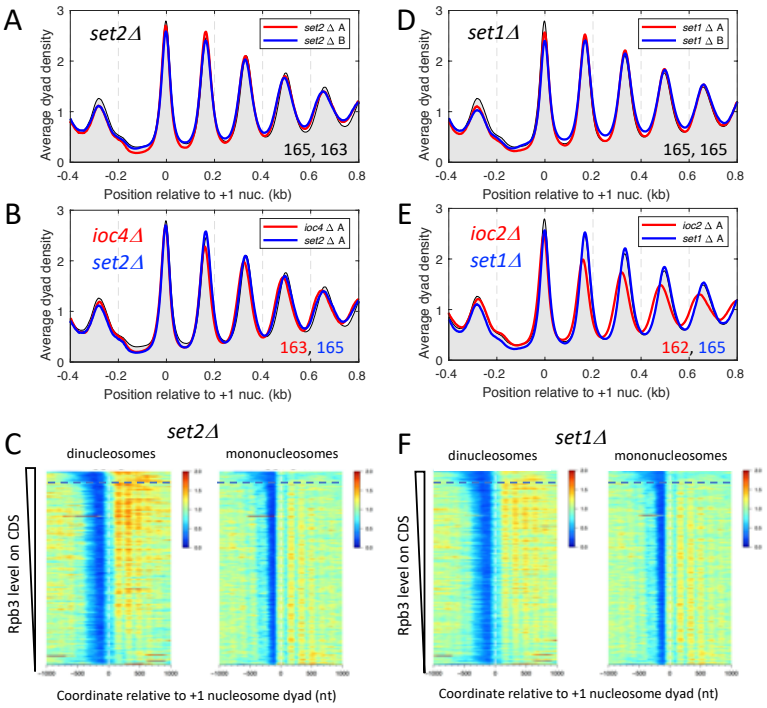

Figure 5. Set2 has a subtle effect on chromatin organization whereas Set1 has no effect. (**A**) Average nucleosome dyad density plot for all genes in *set2Δ* cells. Wild type replicate A is shown as a black line with grey fill. Two biological replicate experiments are shown: A (red line) B (blue line). The average spacing (bp) for replicates A and B are given (bottom right). (**B**) Comparison of chromatin organization in *set2Δ* cells (blue line) and *ioc4Δ* cells (red line) (replicates A). (**C**) Heat map analysis of nucleosome occupancy (coverage) in *set2Δ* cells for all genes aligned on the midpoint of the +1 nucleosome position and sorted by Pol II density on the coding region (CDS). Replicates A are shown (see ***Figure S4*** for replicate B). Dashed line separates the top 300 most active genes from the rest. The scale bar ranges from blue (low nucleosome occupancy) to red (high). Equivalent analyses for cells lacking Set1: (**D**) Average nucleosome dyad density plot for all genes in *set1Δ* cells. (**E**) Chromatin organization in *set1Δ* (blue line) and *ioc2Δ* cells (red line) (replicates A). (**F**) Heat maps of dinucleosome and mononucleosome occupancies in *set1Δ* cells.

Loss of Set1 has no effect on global chromatin organization

The binding of ISW1 to chromatin is mediated through H3-K4 trimethylation by Set1, the only H3-K4 methyltransferase in yeast (***Santos-Rosa et al., 2003***). Since Ioc2 contains a PHD domain (***Smolle et al., 2012***), it might mediate the binding of ISW1b to chromatin. However, we find that chromatin organization in *set1Δ* cells is essentially identical to wild type at the global level (***Figure 5D***) and quite different from that in *ioc2Δ* cells (***Figure 5E***). Dinucleosome distribution in *set1Δ* cells is also similar to wild type cells (***Figure 5F; Figure S3***). Thus, H3-K4me3 is not required for ISW1-dependent nucleosome spacing.

315 **Deletion of the H4 N-terminal tail domain results in shorter nucleosome spacing but does not increase**
316 **dinucleosome levels**
317 Nucleosome mobilisation in vitro by ISWI complexes isolated from different organisms requires the H4
318 N-terminal tail domain, specifically the "basic patch" (residues 16 to 19) (***Clapier et al., 2002, 2001; Yan***
319 ***et al., 2019***). In addition, genetic interactions between *isw1* mutations and H4 mutations (point
320 mutations and a tail deletion) suggest involvement in a common pathway (Lindstrom et al., 2006). We
321 reasoned that deletion of the H4 N-tail might result in a chromatin organization similar to that observed
322 in the *isw1Δ* single mutant: reduced spacing, weaker phasing and increased dinucleosome formation
323 (***Figures 1B and 3A***). We constructed a yeast strain in which both H3/H4 gene loci (*HHT1-HHF1* and
324 *HHT2-HHF2*) were deleted and covered by a plasmid carrying wild type *HHT1-HHF1*, or by *HHT1-*
325 *HHF1Δ21*, in which the first 21 amino acid residues of the H4 N-tail had been deleted. This strain
326 displayed a clear growth phenotype, with a doubling time of ~2.6 h, compared with ~1.8 h for the wild
327 type strain, in synthetic complete (SC) medium. We find that nucleosome spacing is shorter in cells
328 lacking the H4 N-tail (***Figure 6A***), though not quite as short as in *isw1Δ* cells (***Figure 1B***), and both
329 mutants have poor phasing. These observations are consistent with the requirement of Isw1 for the H4
330 N-tail domain. However, removal of the H4 N-tail did not increase dinucleosome prevalence (***Figures 6B***
331 ***and S3***), unlike loss of Isw1 (***Figure 4B***), indicating that loss of Isw1 and loss of the H4 N-tail are not
332 equivalent.

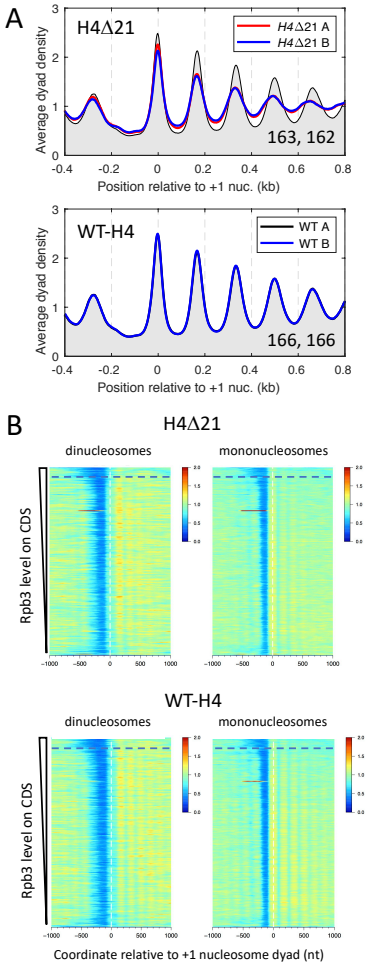

Figure 6. Deletion of the first 21 residues of the H4 N-terminal tail domain results in shorter global nucleosome spacing but no dinucleosome accumulation. **(A)** Comparison of the H4ΔN21 mutant with its isogenic wild type strain (WT-H4) (top panel). WT-H4 replicates (bottom panel). All yeast genes were aligned on the midpoints of their +1 nucleosomes. The dyad distribution was normalised to the global average (set at 1). WT-H4 replicate A: black line with grey fill in both plots. The average spacing in bp is shown for each replicate in the bottom right corner. (**B)** Heat map analysis of nucleosome occupancy (coverage) for all genes aligned on the midpoint of their average +1 nucleosome position and sorted by Pol II density on the coding region (CDS), using ChIP-seq data for the Rpb3 subunit (***Ocampo et al., 2016***). Data for replicate A are shown (see ***Figure S4*** for replicate B). The dashed line separates the top 300 most active genes from the rest. The scale bar is the same for all plots, ranging from blue (low nucleosome occupancy) to red (high occupancy).

333

Discussion

ISW1b is a primary nucleosome spacing enzyme in yeast

We and others have shown previously that Isw1 and Chd1 are both needed for normal global chromatin organization in yeast (***Gkikopoulos et al., 2011; Ocampo et al., 2016***). We proposed that these two enzymes compete to set nucleosome spacing in wild type cells, with Isw1 being dominant, setting wild type spacing, and Chd1 directing shorter spacing (***Ocampo et al., 2016***). In the absence of Isw1, the spacing is short, which we attributed to Chd1 activity. An important complication, which we have addressed here, is that there are two complexes containing the Isw1 ATPase subunit (***Vary et al., 2003***). We have determined their respective roles in chromatin organization in vivo: ISW1b and Chd1 are primarily responsible for global nucleosome spacing in wild type cells, whereas a role for ISW1a in directing intermediate spacing only becomes apparent when ISW1b is absent (***Figure 7A***). We note that INO80 also affects global spacing (***Qiu et al., 2020; van Bakel et al., 2013; Yen et al., 2012***), but it is not yet clear how its activity meshes with that of ISW1b and Chd1.

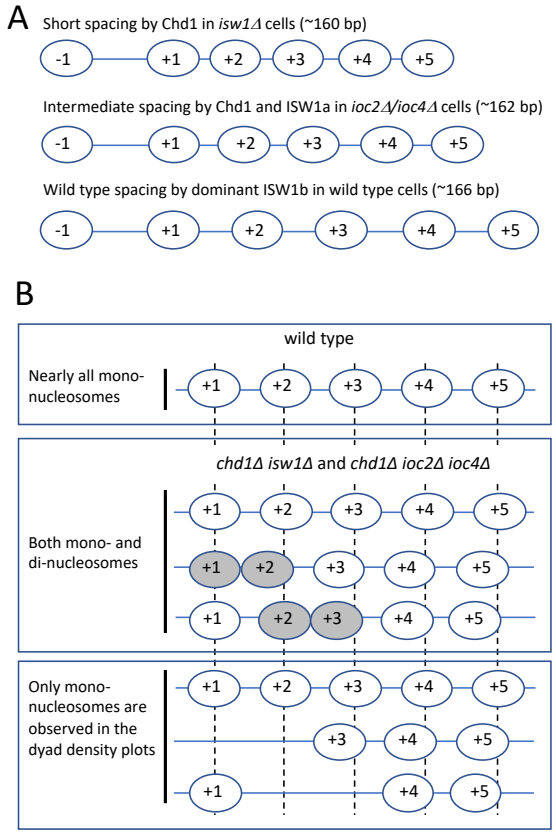

Figure 7. Dominant role of ISW1b in chromatin organization. (**A**) Global average nucleosome spacing is primarily determined by ISW1b (wild type cells), since loss of ISW1a has little effect (*ioc3Δ* mutant). In the absence of ISW1b (*ioc2Δ* and *ioc4Δ* mutants), intermediate spacing is observed, attributed to ISW1a, since the spacing is short in the absence of both ISW1a and ISW1b (*isw1Δ* mutant or *ioc2Δ ioc3Δ ioc4Δ* triple mutant). Short spacing is attributed to Chd1, because the *chd1Δ isw1Δ* double mutant has highly disrupted chromatin.
(**B**) Dinucleosomes disrupt phasing and reduce spacing. Model to show the effects of dinucleosomes on chromatin organization. Top panel: Average nucleosome positions on a gene in wild type cells with regular spacing. Middle: Close-packed dinucleosomes (grey ovals) are high in the absence of both ISW1b and Chd1. These dinucleosomes preferentially involve the +2 nucleosome i.e., they are mostly +1/+2 or +2/+3 dinucleosomes. Nucleosomes farther down the gene (+3 etc.) may be regularly spaced relative to the dinucleosome, but because a linker is missing in the dinucleosome, downstream nucleosomes are out of phase with other nucleosomal arrays, resulting in poor phasing due to interference patterns from the different arrays. Bottom: Dinucleosomes are absent from the mononucleosome dyad density plots, resulting in depressed, flattened peaks. These effects are strongest in cells lacking both ISW1b and Chd1. Dinucleosomes that cannot be resolved by ISW1b can account for shorter spacing in *chd1Δ* cells.

352 A difficulty for our competition model is that, in the absence of Chd1, ISW1b is expected to win
353 the competition, resulting in wild type spacing. Instead, we observe that spacing is somewhat shorter in
354 cells lacking Chd1 (***Ocampo et al., 2016***) (***Figure 2A***). One possible explanation is that the dominance of
355 ISW1b depends on Chd1 and so, in its absence, we see an increased contribution from ISW1a, such that
356 the spacing represents the average of ISW1a and ISW1b activities. If so, cells having only ISW1b (the
357 *chd1Δ ioc3Δ* double mutant) are expected to have wild type spacing. However, the result is intermediate
358 spacing, very similar to the *chd1Δ* single mutant (***Figure 2***). Alternatively, ISW1b might only be able to
359 create nucleosome arrays with wild type spacing if Chd1 has already made arrays with short spacing,
360 although this model is inconsistent with in vitro data showing that purified ISW1b can space
361 nucleosomes by itself (***Vary et al., 2003***).
362 A more satisfying explanation involves dinucleosomes (***Figure 7B***). Consider a single gene. If
363 there are regularly spaced nucleosomes downstream of a close-packed +1/+2 dinucleosome (i.e. no
364 linker), these nucleosomes will be out of phase by one linker length with nucleosomes in cells with no
365 dinucleosome on this gene. Other cells may have a +2/+3 dinucleosome instead, which will alter the
366 positions of regularly spaced downstream nucleosomes to give a different phasing. The result is
367 generally weaker phasing (peak flattening) and a shift to shorter average spacing. Moreover, since the
368 dinucleosomes are not counted in the mononucleosome phasing pattern, there will be missing
369 occupancy around the +2 nucleosome, resulting in more pattern disruption (primarily a depressed +2
370 nucleosome peak). These effects will increase as the fraction of genes having a dinucleosome increases:
371 the *chd1Δ isw1Δ* double mutant and the *chd1Δ ioc2Δ ioc4Δ* triple mutant both have high dinucleosome
372 levels and extremely poor phasing. The *chd1Δ* single mutant has fewer dinucleosomes, resulting in a
373 smaller shift in the peaks to shorter spacing. These considerations can account for the shift to shorter
374 spacing in the absence of Chd1 and for the major disruption of chromatin in the absence of both Chd1
375 and ISW1b. Thus, we propose that the spacing is shorter in cells lacking Chd1 because ISW1b cannot
376 resolve all of the dinucleosomes.
377
378 **Dinucleosome levels correlate with Pol II levels**
379 Previously, we showed that Isw1 and/or Chd1 is required to resolve dinucleosomes, or to prevent their
380 formation (***Ocampo et al., 2019***). Here we show that both enzymes are important for separating
381 dinucleosomes and that, as observed for spacing activity, ISW1b is much more important than ISW1a. In
382 vitro, both ISW1a and ISW1b can move nucleosomes reconstituted on a pair of 601 nucleosome
383 positioning sequences farther apart, even if separated by a linker of only 4 bp (***Krajewski, 2014***),
384 indicating that both ISW1 complexes probably have close-packed dinucleosome resolving activity.
385 Interestingly, SWI/SNF may also be able to resolve dinucleosomes (***Dechassa et al., 2010***).
386 We observe a correlation between dinucleosome and Pol II levels on genes, such that the least
387 active genes have fewer dinucleosomes. The top ~300 most active genes represent an exception in that
388 they are only modestly enriched in dinucleosomes, relative to the genes immediately below them in the
389 heat map, which we attribute to the nucleosome loss that occurs at the most active genes (***Cole et al.,***
390 ***2014; Schwabish and Struhl, 2007, 2004***). This loss may include both mononucleosomes and
391 dinucleosomes. There is an interesting conundrum concerning these most active genes, since they have
392 both very short nucleosome spacing (roughly ~155 bp), which implies that more nucleosomes are
393 present on a gene of a given length, and reduced nucleosome occupancy, which indicates fewer

394 nucleosomes. A possible resolution is that these genes have fewer nucleosomes which form clusters
395 with short spacing separated by gaps (i.e., long linkers).
396 The correlation between dinucleosomes and transcriptional activity suggests that Pol II might
397 form dinucleosomes as it transcribes along a gene, perhaps as part of a general tendency to push
398 nucleosomes closer together during transcription, possibly to free up the space needed for the Pol II
399 elongation complex itself, since the average linker is only ~20 bp. Some support for this hypothesis
400 comes from the observation that nucleosome spacing is longer in non-transcribing yeast cells than in
401 wild type cells (this experiment was possible using the Pol II large subunit *rpb1-1* mutant at the non-
402 permissive temperature) (***Weiner et al., 2010***), suggesting that transcription shortens spacing, although
403 the effect could be indirect.
404 In summary, we propose that transcription may result in some nucleosome loss, and some
405 clustering of the remaining nucleosomes with short spacing, including some close-packed
406 dinucleosomes. ISW1b and Chd1 are needed to space the nucleosomes out again after transcription.
407 Once a gene is transcribed, its chromatin organization is not restored if ISW1b and Chd1 are absent. It
408 seems likely that dinucleosomes might interfere with transcription and other processes. If so, regulating
409 dinucleosome formation might represent a novel mechanism for control of gene expression.
410
411 **The Set2 methyltransferase makes a subtle contribution to global chromatin organization**
412 We observe that the ancillary subunits of ISW1b, Ioc2 and Ioc4, are both necessary for ISW1b-
413 dependent chromatin organization, although Ioc2 makes a greater contribution, since it affects phasing
414 as well as spacing. We suggest that Ioc2 and Ioc4 cooperate to influence the remodeling activity of the
415 Isw1 subunit. Both are linked to certain histone modifications. Ioc4 binds to an H3-K36me3 peptide with
416 higher affinity than the unmethylated peptide, suggesting that Set2-mediated H3-K36me3 might be an
417 important regulator of ISW1b (***Maltby et al., 2012; Smolle et al., 2012; Smolle and Workman, 2013***).
418 Our data provide some evidence to support this proposal, because loss of Set2 has a similar but weaker
419 effect on chromatin organization as loss of Ioc4, although they are not quite equivalent.
420 Ioc2 has a PHD domain (***Smolle et al., 2012***) which binds H3-K4me3, accounting for the H3-
421 K4me3/Set1-dependence of Isw1 binding to chromatin at a subset of genes (***Santos-Rosa et al., 2003***).
422 However, our data indicate that the nucleosome spacing activity of the ISW1b complex, which requires
423 Isw1 binding to chromatin, is independent of Set1 (and therefore of H3-K4me3) at the global level, since
424 cells lacking Set1 have normal chromatin organization. We also note that, since loss of Set1 did not
425 result in global chromatin defects, the binding of Chd1 to H3K4me3 through one of its chromodomains
426 (***Pray-Grant et al., 2005***) is not critical for its nucleosome spacing function.
427 We note that neither ISW1 complex requires H3-K4me3 or H3-K36me3 to space nucleosomes in
428 vitro, since they are active on nucleosomes containing unmodified recombinant histones. On the other
429 hand, in vivo, H3-K36me3 and H3-K4me3 may have local effects on ISW1b activity, rather than global
430 effects, which we have not detected. These are probably not occurring at the most active genes because
431 their chromatin organization in *set1Δ* and *set2Δ* cells is similar to wild type (***Figure S2C***). Alternatively,
432 H3-K36me3 and H3-K4me3 recognition may affect other functions of ISW1b, such as gene repression
433 (***Pinskaya et al., 2009***) or mRNP quality control (***Babour et al., 2016***).
434
435

436 **The H4 N-terminal tail domain is required for normal nucleosome spacing**
437 The H4 tail domain is generally required by ISWI-like enzymes for activity (***Clapier et al., 2017, 2001;***
438 ***Hamiche et al., 2001; Paul and Bartholomew, 2018***). The ISWI ATPase subunit has an inhibitory AutoN
439 domain that resembles the H4 tail, which is displaced by the H4 tail when ISWI binds to a nucleosome
440 (***Clapier et al., 2017; Paul and Bartholomew, 2018***). The isolated yeast Isw1 subunit is inactive without
441 Ioc subunits unless the AutoN domain is inactivated by mutation (***Yan et al., 2019***), implying that the Ioc
442 subunits may regulate Isw1 activity through the AutoN domain. We find that the H4 tail deletion mutant
443 exhibits shorter spacing, consistent with inactivation of ISW1b, but there is no increase in
444 dinucleosomes. The most likely explanation for the non-equivalence of the H4Δ21 and *isw1Δ* mutations
445 is that the H4 tail domain is involved in multiple processes, including interactions with other remodelers
446 and proteins. This possibility is supported by the fact that the H4Δ21 mutant has a strong growth defect,
447 unlike the various *ioc* mutants. Since Chd1 also makes contacts with the basic patch in the H4 tail
448 (***Ferreira et al., 2007; Sundaramoorthy et al., 2018***), its remodeling activity may also be compromised,
449 although its chromatin is clearly not as disrupted as in the *chd1Δ isw1Δ* double mutant. The H4 N-tail is
450 also required by ISW2 in vitro (***Dang et al., 2006***), although global chromatin organization is unaffected
451 in *isw2Δ* cells (***Gkikopoulos et al., 2011; Ocampo et al., 2016***). The low prevalence of dinucleosomes in
452 the H4Δ21 mutant suggests that the H4 tail might be required for dinucleosome formation, possibly
453 because the increased negative charge on nucleosomes lacking the H4 tail might limit how closely
454 nucleosomes can approach one another (***Blank and Becker, 1995; Clark and Kimura, 1990***). Deletion of
455 the H4 tail also results in the loss of multiple post-translational modification sites, preventing interaction
456 with many chromatin factors.
457

Materials and methods

Plasmid construction. The primers used in this study are listed in ***Table S1***. pRS-HHT1-HHF1 (p368) was constructed by insertion of the 1930-bp SacI-PstI fragment containing the *HHT1-HHF1* locus from p367 (***Eriksson et al., 2005***) at the same sites in pRS317 (*CEN ARS LYS2*) (ATCC 77157). pRS-HHT1-HHF1Δ21 (p730) was constructed by replacing the 752-bp AfeI-SacI fragment in p368 with a 689-bp AfeI-SacI fragment with the H4 N-terminal tail deletion (H4 begins Met-Leu22…) made by ligating two PCR fragments together (obtained using p368 as template with primers 1770/1771 and 1773/1812). The sequence was confirmed.

Yeast strain construction. The yeast strains used in this study are listed in ***Table S2***. YDC507 (H4 N-terminal tail deletion) was constructed by transforming ROY1281 (***Dhillon and Kamakaka, 2000***), which carries plasmid pCC67 (2 micron origin *URA3 HHT1-HHT1 HTA1-HTB1*) (***Clark-Adams et al., 1988***), with p730 (*CEN ARS LYS2 HHT1-HHF1Δ21*), selection on plates made with synthetic complete medium without lysine (SC-lys) and then counter-selection against *URA3* with 5-fluoro-orotic acid (5-FOA) to evict pCC67. A wild type control strain (YDC101) was constructed in the same way using p368 (*CEN ARS LYS2 HHT1-HHF1*) instead of p730. The diploid strain YPE600 was made by crossing YTT196 (***Tsukiyama et al., 1999***) with YDC111 (***Kim et al., 2006***). YPE606 (*ioc3Δ*) was constructed by transforming YPE600 with an *ioc3Δ::KanMX* fragment made using primers 1918/1919 and genomic DNA from YTT645, followed by G418 selection on YPD plates and sporulation. YPE608 (*ioc4Δ*) was constructed by transforming YPE600 with an *ioc4Δ::HPH1* fragment made using primers 1922/1923 and genomic DNA from YTT827, followed by hygromycin selection on YPD plates and sporulation. YPE636 (*ioc2Δ*) was constructed by transforming YPE600 with an *ioc2Δ::URA3* fragment made using primers 1961/1962 and extended using primers 1965/1966 and wild type genomic DNA as template, followed by selection on SC-ura plates and sporulation. YPE654 (*ioc2Δ ioc3Δ*) was constructed by transforming YPE636 with the *ioc3Δ::KanMX* DNA fragment (see above). YPE655 (*ioc2Δ ioc4Δ*) was constructed by transforming YPE636 with the *ioc4Δ::HPH1* fragment (see above). YPE657 (*ioc2Δ ioc3Δ ioc4Δ*) was constructed by transforming YPE654 with the *ioc4Δ::HPH1* fragment. YPE712 (*chd1Δ ioc3Δ*) was obtained by crossing YJO486 (***Ocampo et al., 2016***) with YPE607. YJO487 was obtained by sporulation of YJO505 (***Ocampo et al., 2016***). YPE715 (*chd1Δ ioc2Δ ioc4Δ*) was constructed by crossing YJO487 with YPE655. YPE602 (*set1Δ*) was constructed by transforming YPE600 with a *set1Δ::NAT1* fragment made using primers 1926/1927 and genomic DNA from YTT1986, followed by nourseothricin selection on YPD plates and sporulation. YPE604 (*set2Δ*) was constructed by transforming YDC111 with a *set2Δ::TRP1* fragment made using primers 1914/1915 extended with 1916/17 and plasmid pFA6a-TRP1 (***Longtine et al., 1998***), followed by selection on SC-trp plates.

MNase-seq: Nuclei were prepared as described (***Cole et al., 2011***). MNase digestion of nuclei and construction of paired-end libraries was as described (***Chereji et al., 2017***), except that mononucleosomal DNA was not gel-purified, in order to retain mononucleosomes and dinucleosomes in the correct proportions (***Ocampo et al., 2019***). Biological replicate experiments were performed for all strains. MNase-seq data were analysed using scripts described by (***Ocampo et al., 2019***). Sequence data

499 for YJO484 (*chd1Δ isw1Δ*) are available at the GEO database (GSE117514 (***Ocampo et al., 2019***)). The
500 sequence data from this study have been submitted to the NCBI Gene Expression Omnibus (GEO;
501 http://www.ncbi.nlm.nih.gov/geo/) under accession number GSE156224.
502

503 ## Acknowledgements

504 We thank Alan Hinnebusch for helpful comments on the manuscript and Răzvan Chereji for help with
505 the bioinformatics. We thank Alex Naim for constructing p368, Toshi Tsukiyama for yeast strains, and
506 Rohinton Kamakaka and Namrita Dhillon for pCC67 (pRO149) and ROY1281. This research was
507 supported by the Intramural Research Program of the NIH (NICHD). We thank the NHLBI Core Facility
508 (Yan Luo, Poching Liu, and Jun Zhu) for paired-end sequencing. This study utilized the high performance
509 computational capabilities of the Biowulf Linux cluster at the National Institutes of Health.
510

511 ## References

512

513 Babour, A., Shen, Q., Dos-Santos, J., Murray, S., Gay, A., Challal, D., Fasken, M., Palancade, B., Corbett,
514 A., Libri, D., Mellor, J., Dargemont, C., 2016. The Chromatin Remodeler ISW1 Is a Quality Control
515 Factor that Surveys Nuclear mRNP Biogenesis. Cell 167, 1201-1214.e15.
516 doi:10.1016/j.cell.2016.10.048
517 Barisic, D., Stadler, M.B., Iurlaro, M., Schübeler, D., 2019. Mammalian ISWI and SWI/SNF selectively
518 mediate binding of distinct transcription factors. Nature 569, 136–140. doi:10.1038/s41586-019-
519 1115-5
520 Blank, T.A., Becker, P.B., 1995. Electrostatic mechanism of nucleosome spacing. J. Mol. Biol. 252, 305–
521 313. doi:10.1006/jmbi.1995.0498
522 Chereji, R.V., Clark, D.J., 2018. Major determinants of nucleosome positioning. Biophys. J. 114, 2279–
523 2289. doi:10.1016/j.bpj.2018.03.015
524 Chereji, R.V., Ocampo, J., Clark, D.J., 2017. MNase-Sensitive Complexes in Yeast: Nucleosomes and Non-
525 histone Barriers. Mol. Cell 65, 565-577.e3. doi:10.1016/j.molcel.2016.12.009
526 Clapier, C.R., Iwasa, J., Cairns, B.R., Peterson, C.L., 2017. Mechanisms of action and regulation of ATP-
527 dependent chromatin-remodelling complexes. Nat. Rev. Mol. Cell Biol. 18, 407–422.
528 doi:10.1038/nrm.2017.26
529 Clapier, C.R., Längst, G., Corona, D.F., Becker, P.B., Nightingale, K.P., 2001. Critical role for the histone H4
530 N terminus in nucleosome remodeling by ISWI. Mol. Cell. Biol. 21, 875–883.
531 doi:10.1128/MCB.21.3.875-883.2001
532 Clapier, C.R., Nightingale, K.P., Becker, P.B., 2002. A critical epitope for substrate recognition by the
533 nucleosome remodeling ATPase ISWI. Nucleic Acids Res. 30, 649–655. doi:10.1093/nar/30.3.649
534 Clark, D.J., Kimura, T., 1990. Electrostatic mechanism of chromatin folding. J. Mol. Biol. 211, 883–896.
535 doi:10.1016/0022-2836(90)90081-V
536 Cole, H.A., Howard, B.H., Clark, D.J., 2011. Activation-induced disruption of nucleosome position clusters
537 on the coding regions of Gcn4-dependent genes extends into neighbouring genes. Nucleic Acids
538 Res. 39, 9521–9535. doi:10.1093/nar/gkr643
539 Cole, H.A., Ocampo, J., Iben, J.R., Chereji, R.V., Clark, D.J., 2014. Heavy transcription of yeast genes

540 correlates with differential loss of histone H2B relative to H4 and queued RNA polymerases. Nucleic
541 Acids Res. 42, 12512–12522. doi:10.1093/nar/gku1013
542 Cui, F., Cole, H.A., Clark, D.J., Zhurkin, V.B., 2012. Transcriptional activation of yeast genes disrupts
543 intragenic nucleosome phasing. Nucleic Acids Res. 40, 10753–10764. doi:10.1093/nar/gks870
544 Dang, W., Kagalwala, M.N., Bartholomew, B., 2006. Regulation of ISW2 by concerted action of histone
545 H4 tail and extranucleosomal DNA. Mol. Cell. Biol. 26, 7388–7396. doi:10.1128/MCB.01159-06
546 Dechassa, M.L., Sabri, A., Pondugula, S., Kassabov, S.R., Chatterjee, N., Kladde, M.P., Bartholomew, B.,
547 2010. SWI/SNF has intrinsic nucleosome disassembly activity that is dependent on adjacent
548 nucleosomes. Mol. Cell 38, 590–602. doi:10.1016/j.molcel.2010.02.040
549 Dhillon, N., Kamakaka, R.T., 2000. A histone variant, Htz1p, and a Sir1p-like protein, Esc2p, mediate
550 silencing at HMR. Mol. Cell 6, 769–780. doi:10.1016/s1097-2765(00)00076-9
551 Eriksson, P.R., Mendiratta, G., McLaughlin, N.B., Wolfsberg, T.G., Mariño-Ramírez, L., Pompa, T.A.,
552 Jainerin, M., Landsman, D., Shen, C.-H., Clark, D.J., 2005. Global regulation by the yeast Spt10
553 protein is mediated through chromatin structure and the histone upstream activating sequence
554 elements. Mol. Cell. Biol. 25, 9127–9137. doi:10.1128/MCB.25.20.9127-9137.2005
555 Ferreira, H., Flaus, A., Owen-Hughes, T., 2007. Histone modifications influence the action of Snf2 family
556 remodelling enzymes by different mechanisms. J. Mol. Biol. 374, 563–579.
557 doi:10.1016/j.jmb.2007.09.059
558 Gangaraju, V.K., Bartholomew, B., 2007. Dependency of ISW1a chromatin remodeling on
559 extranucleosomal DNA. Mol. Cell. Biol. 27, 3217–3225. doi:10.1128/MCB.01731-06
560 Gkikopoulos, T., Schofield, P., Singh, V., Pinskaya, M., Mellor, J., Smolle, M., Workman, J.L., Barton, G.J.,
561 Owen-Hughes, T., 2011. A role for Snf2-related nucleosome-spacing enzymes in genome-wide
562 nucleosome organization. Science 333, 1758–1760. doi:10.1126/science.1206097
563 Hamiche, A., Kang, J.G., Dennis, C., Xiao, H., Wu, C., 2001. Histone tails modulate nucleosome mobility
564 and regulate ATP-dependent nucleosome sliding by NURF. Proc Natl Acad Sci USA 98, 14316–
565 14321. doi:10.1073/pnas.251421398
566 Ito, T., Bulger, M., Pazin, M.J., Kobayashi, R., Kadonaga, J.T., 1997. ACF, an ISWI-containing and ATP-
567 utilizing chromatin assembly and remodeling factor. Cell 90, 145–155. doi:10.1016/s0092-
568 8674(00)80321-9
569 Kim, Y., McLaughlin, N., Lindstrom, K., Tsukiyama, T., Clark, D.J., 2006. Activation of Saccharomyces
570 cerevisiae HIS3 results in Gcn4p-dependent, SWI/SNF-dependent mobilization of nucleosomes over
571 the entire gene. Mol. Cell. Biol. 26, 8607–8622. doi:10.1128/MCB.00678-06
572 Krajewski, W.A., 2014. Yeast Isw1a and Isw1b exhibit similar nucleosome mobilization capacities for
573 mononucleosomes, but differently mobilize dinucleosome templates. Arch. Biochem. Biophys. 546,
574 72–80. doi:10.1016/j.abb.2014.02.003
575 Krietenstein, N., Wal, M., Watanabe, S., Park, B., Peterson, C.L., Pugh, B.F., Korber, P., 2016. Genomic
576 Nucleosome Organization Reconstituted with Pure Proteins. Cell 167, 709-721.e12.
577 doi:10.1016/j.cell.2016.09.045
578 Lafon, A., Petty, E., Pillus, L., 2012. Functional antagonism between Sas3 and Gcn5 acetyltransferases
579 and ISWI chromatin remodelers. PLoS Genet. 8, e1002994. doi:10.1371/journal.pgen.1002994
580 Lieleg, C., Ketterer, P., Nuebler, J., Ludwigsen, J., Gerland, U., Dietz, H., Mueller-Planitz, F., Korber, P.,
581 2015. Nucleosome spacing generated by ISWI and CHD1 remodelers is constant regardless of

582 nucleosome density. Mol. Cell. Biol. 35, 1588–1605. doi:10.1128/MCB.01070-14
583 Lindstrom, K.C., Vary, J.C., Parthun, M.R., Delrow, J., Tsukiyama, T., 2006. Isw1 functions in parallel with
584 the NuA4 and Swr1 complexes in stress-induced gene repression. Mol. Cell. Biol. 26, 6117–6129.
585 doi:10.1128/MCB.00642-06
586 Longtine, M.S., McKenzie, A., Demarini, D.J., Shah, N.G., Wach, A., Brachat, A., Philippsen, P., Pringle,
587 J.R., 1998. Additional modules for versatile and economical PCR-based gene deletion and
588 modification in Saccharomyces cerevisiae. Yeast 14, 953–961. doi:10.1002/(SICI)1097-
589 0061(199807)14:10<953::AID-YEA293>3.0.CO;2-U
590 Luger, K., Mäder, A.W., Richmond, R.K., Sargent, D.F., Richmond, T.J., 1997. Crystal structure of the
591 nucleosome core particle at 2.8 A resolution. Nature 389, 251–260. doi:10.1038/38444
592 Lusser, A., Urwin, D.L., Kadonaga, J.T., 2005. Distinct activities of CHD1 and ACF in ATP-dependent
593 chromatin assembly. Nat. Struct. Mol. Biol. 12, 160–166. doi:10.1038/nsmb884
594 Maltby, V.E., Martin, B.J.E., Schulze, J.M., Johnson, I., Hentrich, T., Sharma, A., Kobor, M.S., Howe, L.,
595 2012. Histone H3 lysine 36 methylation targets the Isw1b remodeling complex to chromatin. Mol.
596 Cell. Biol. 32, 3479–3485. doi:10.1128/MCB.00389-12
597 Mellor, J., Morillon, A., 2004. ISWI complexes in Saccharomyces cerevisiae. Biochim. Biophys. Acta 1677,
598 100–112. doi:10.1016/j.bbaexp.2003.10.014
599 Morillon, A., Karabetsou, N., O'Sullivan, J., Kent, N., Proudfoot, N., Mellor, J., 2003. Isw1 chromatin
600 remodeling ATPase coordinates transcription elongation and termination by RNA polymerase II.
601 Cell 115, 425–435. doi:10.1016/s0092-8674(03)00880-8
602 Ocampo, J., Chereji, R.V., Eriksson, P.R., Clark, D.J., 2016. The ISW1 and CHD1 ATP-dependent chromatin
603 remodelers compete to set nucleosome spacing in vivo. Nucleic Acids Res. 44, 4625–4635.
604 doi:10.1093/nar/gkw068
605 Ocampo, J., Chereji, R.V., Eriksson, P.R., Clark, D.J., 2019. Contrasting roles of the RSC and ISW1/CHD1
606 chromatin remodelers in RNA polymerase II elongation and termination. Genome Res. 29, 407–417.
607 doi:10.1101/gr.242032.118
608 Paul, S., Bartholomew, B., 2018. Regulation of ATP-dependent chromatin remodelers:
609 accelerators/brakes, anchors and sensors. Biochem. Soc. Trans. 46, 1423–1430.
610 doi:10.1042/BST20180043
611 Pinskaya, M., Nair, A., Clynes, D., Morillon, A., Mellor, J., 2009. Nucleosome remodeling and
612 transcriptional repression are distinct functions of Isw1 in Saccharomyces cerevisiae. Mol. Cell. Biol.
613 29, 2419–2430. doi:10.1128/MCB.01050-08
614 Pointner, J., Persson, J., Prasad, P., Norman-Axelsson, U., Strålfors, A., Khorosjutina, O., Krietenstein, N.,
615 Svensson, J.P., Ekwall, K., Korber, P., 2012. CHD1 remodelers regulate nucleosome spacing in vitro
616 and align nucleosomal arrays over gene coding regions in S. pombe. EMBO J. 31, 4388–4403.
617 doi:10.1038/emboj.2012.289
618 Prajapati, H.K., Ocampo, J., Clark, D.J., 2020. Interplay among ATP-Dependent Chromatin Remodelers
619 Determines Chromatin Organization in Yeast. Biology (Basel) 9. doi:10.3390/biology9080190
620 Pray-Grant, M.G., Daniel, J.A., Schieltz, D., Yates, J.R., Grant, P.A., 2005. Chd1 chromodomain links
621 histone H3 methylation with SAGA- and SLIK-dependent acetylation. Nature 433, 434–438.
622 doi:10.1038/nature03242
623 Qiu, H., Biernat, E., Govind, C.K., Rawal, Y., Chereji, R.V., Clark, D.J., Hinnebusch, A.G., 2020. Chromatin

624 remodeler Ino80C acts independently of H2A.Z to evict promoter nucleosomes and stimulate
625 transcription of highly expressed genes in yeast. Nucleic Acids Res. doi:10.1093/nar/gkaa571
626 Richmond, T.J., 2012. Nucleosome recognition and spacing by chromatin remodelling factor ISW1a.
627 Biochem. Soc. Trans. 40, 347–350. doi:10.1042/BST20110748
628 Santos-Rosa, H., Schneider, R., Bernstein, B.E., Karabetsou, N., Morillon, A., Weise, C., Schreiber, S.L.,
629 Mellor, J., Kouzarides, T., 2003. Methylation of histone H3 K4 mediates association of the Isw1p
630 ATPase with chromatin. Mol. Cell 12, 1325–1332. doi:10.1016/s1097-2765(03)00438-6
631 Schwabish, M.A., Struhl, K., 2004. Evidence for eviction and rapid deposition of histones upon
632 transcriptional elongation by RNA polymerase II. Mol. Cell. Biol. 24, 10111–10117.
633 doi:10.1128/MCB.24.23.10111-10117.2004
634 Schwabish, M.A., Struhl, K., 2007. The Swi/Snf complex is important for histone eviction during
635 transcriptional activation and RNA polymerase II elongation in vivo. Mol. Cell. Biol. 27, 6987–6995.
636 doi:10.1128/MCB.00717-07
637 Simic, R., Lindstrom, D.L., Tran, H.G., Roinick, K.L., Costa, P.J., Johnson, A.D., Hartzog, G.A., Arndt, K.M.,
638 2003. Chromatin remodeling protein Chd1 interacts with transcription elongation factors and
639 localizes to transcribed genes. EMBO J. 22, 1846–1856. doi:10.1093/emboj/cdg179
640 Smolle, M., Venkatesh, S., Gogol, M.M., Li, H., Zhang, Y., Florens, L., Washburn, M.P., Workman, J.L.,
641 2012. Chromatin remodelers Isw1 and Chd1 maintain chromatin structure during transcription by
642 preventing histone exchange. Nat. Struct. Mol. Biol. 19, 884–892. doi:10.1038/nsmb.2312
643 Smolle, M., Workman, J.L., 2013. Transcription-associated histone modifications and cryptic
644 transcription. Biochim. Biophys. Acta 1829, 84–97. doi:10.1016/j.bbagrm.2012.08.008
645 Stockdale, C., Flaus, A., Ferreira, H., Owen-Hughes, T., 2006. Analysis of nucleosome repositioning by
646 yeast ISWI and Chd1 chromatin remodeling complexes. J. Biol. Chem. 281, 16279–16288.
647 doi:10.1074/jbc.M600682200
648 Sundaramoorthy, R., Hughes, A.L., El-Mkami, H., Norman, D.G., Ferreira, H., Owen-Hughes, T., 2018.
649 Structure of the chromatin remodelling enzyme Chd1 bound to a ubiquitinylated nucleosome. elife
650 7. doi:10.7554/eLife.35720
651 Thoma, F., Koller, T., Klug, A., 1979. Involvement of histone H1 in the organization of the nucleosome
652 and of the salt-dependent superstructures of chromatin. J. Cell Biol. 83, 403–427.
653 doi:10.1083/jcb.83.2.403
654 Tirosh, I., Sigal, N., Barkai, N., 2010. Widespread remodeling of mid-coding sequence nucleosomes by
655 Isw1. Gen. Biol. 11:R49. doi:10.1186/gb-2010-11-5-r49
656 Torigoe, S.E., Patel, A., Khuong, M.T., Bowman, G.D., Kadonaga, J.T., 2013. ATP-dependent chromatin
657 assembly is functionally distinct from chromatin remodeling. elife 2, e00863.
658 doi:10.7554/eLife.00863
659 Tsukiyama, T., Palmer, J., Landel, C.C., Shiloach, J., Wu, C., 1999. Characterization of the imitation switch
660 subfamily of ATP-dependent chromatin-remodeling factors in Saccharomyces cerevisiae. Genes
661 Dev. 13, 686–697. doi:10.1101/gad.13.6.686
662 Udugama, M., Sabri, A., Bartholomew, B., 2011. The INO80 ATP-dependent chromatin remodeling
663 complex is a nucleosome spacing factor. Mol. Cell. Biol. 31, 662–673. doi:10.1128/MCB.01035-10
664 van Bakel, H., Tsui, K., Gebbia, M., Mnaimneh, S., Hughes, T.R., Nislow, C., 2013. A compendium of
665 nucleosome and transcript profiles reveals determinants of chromatin architecture and

666 transcription. PLoS Genet. 9, e1003479. doi:10.1371/journal.pgen.1003479
667 Vary, J.C., Fazzio, T.G., Tsukiyama, T., 2004. Assembly of yeast chromatin using ISWI complexes. Meth.
668 Enzymol. 375, 88–102.
669 Vary, J.C., Gangaraju, V.K., Qin, J., Landel, C.C., Kooperberg, C., Bartholomew, B., Tsukiyama, T., 2003.
670 Yeast Isw1p forms two separable complexes in vivo. Mol. Cell. Biol. 23, 80–91.
671 doi:10.1128/mcb.23.1.80-91.2003
672 Weiner, A., Hughes, A., Yassour, M., Rando, O.J., Friedman, N., 2010. High-resolution nucleosome
673 mapping reveals transcription-dependent promoter packaging. Genome Res. 20, 90–100.
674 doi:10.1101/gr.098509.109
675 Wiechens, N., Singh, V., Gkikopoulos, T., Schofield, P., Rocha, S., Owen-Hughes, T., 2016. The Chromatin
676 Remodelling Enzymes SNF2H and SNF2L Position Nucleosomes adjacent to CTCF and Other
677 Transcription Factors. PLoS Genet. 12, e1005940. doi:10.1371/journal.pgen.1005940
678 Yamada, K., Frouws, T.D., Angst, B., Fitzgerald, D.J., DeLuca, C., Schimmele, K., Sargent, D.F., Richmond,
679 T.J., 2011. Structure and mechanism of the chromatin remodelling factor ISW1a. Nature 472, 448–
680 453. doi:10.1038/nature09947
681 Yan, L., Wu, H., Li, X., Gao, N., Chen, Z., 2019. Structures of the ISWI-nucleosome complex reveal a
682 conserved mechanism of chromatin remodeling. Nat. Struct. Mol. Biol. 26, 258–266.
683 doi:10.1038/s41594-019-0199-9
684 Yen, K., Vinayachandran, V., Batta, K., Koerber, R.T., Pugh, B.F., 2012. Genome-wide nucleosome
685 specificity and directionality of chromatin remodelers. Cell 149, 1461–1473.
686 doi:10.1016/j.cell.2012.04.036
687 Zhao, X., Muller, E.G., Rothstein, R., 1998. A suppressor of two essential checkpoint genes identifies a
688 novel protein that negatively affects dNTP pools. Mol. Cell 2, 329–340. doi:10.1016/s1097-
689 2765(00)80277-4

690 **Supplementary Figures**

691

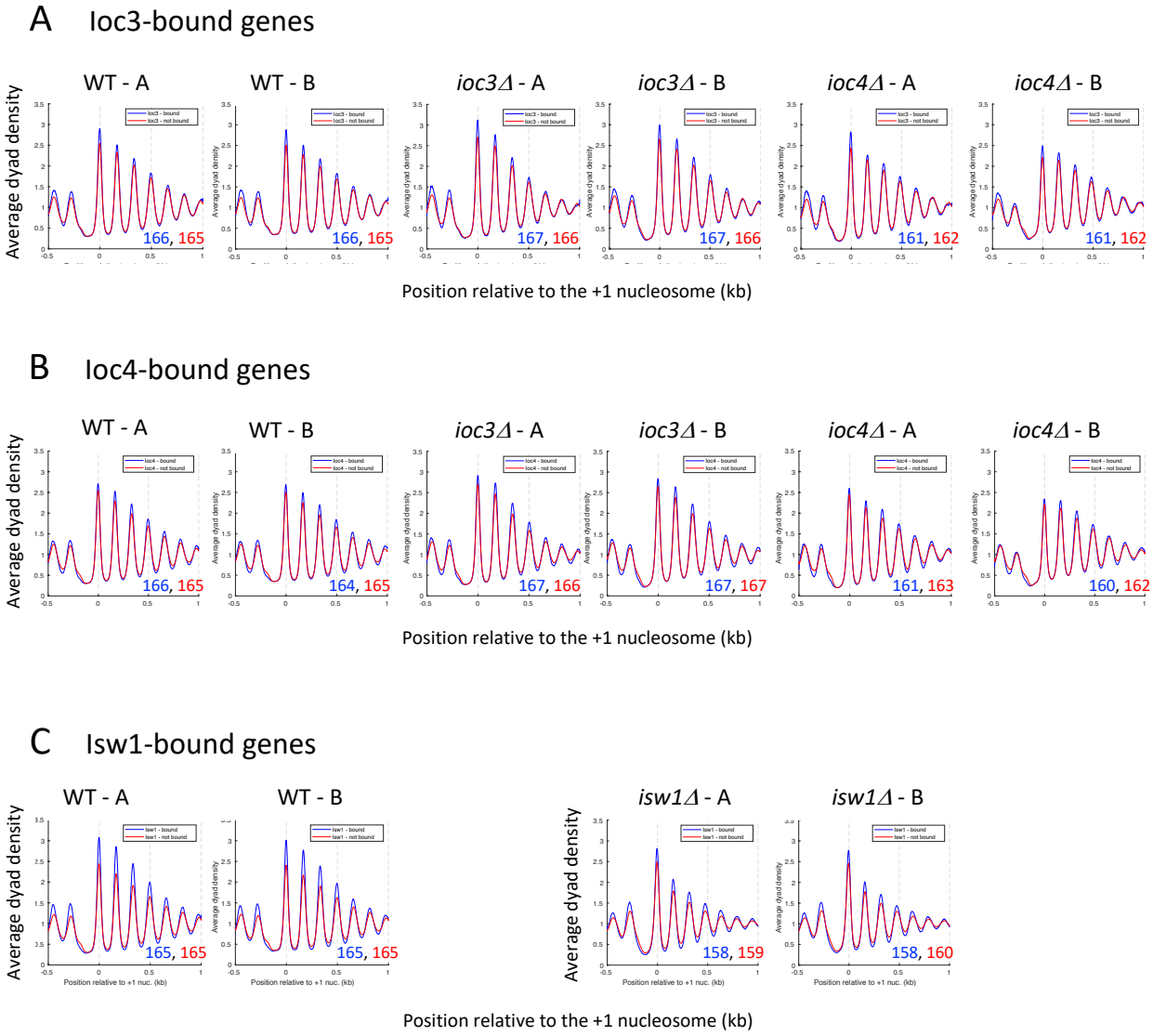

692
693

694 **Figure S1.** The chromatin organizations of Ioc3-bound, Ioc4-bound and Isw1-bound genes are not
695 significantly different from the unbound genes. Target genes for ISW1a (Ioc3-bound), ISW1b (Ioc4-
696 bound) and both complexes (Isw1-bound) are defined by ChIP-seq data (***Yen et al., 2012***). Average
697 nucleosome dyad density plots for bound and unbound genes: (**A**) Ioc3-bound (blue line) and non-bound
698 (red line) genes in wild type (WT) and *ioc3Δ* cells. (**B**) Ioc4-bound (blue line) and non-bound (red line)
699 genes in WT and *ioc4Δ* cells. (**C**) Isw1-bound (blue line) and non-bound (red line) genes in WT and *isw1Δ*
700 cells. All 5770 yeast genes were aligned on the midpoints of their +1 nucleosomes. The dyad distribution
701 was normalized to the global average (set at 1). Two biological replicate experiments (A and B) are
702 shown. The average spacing in bp is shown for bound genes (blue text) and non-bound genes (red text)
703 in the bottom right corner (measured by regression analysis of the first 5 nucleosome peaks, beginning
704 with the +1 nucleosome).

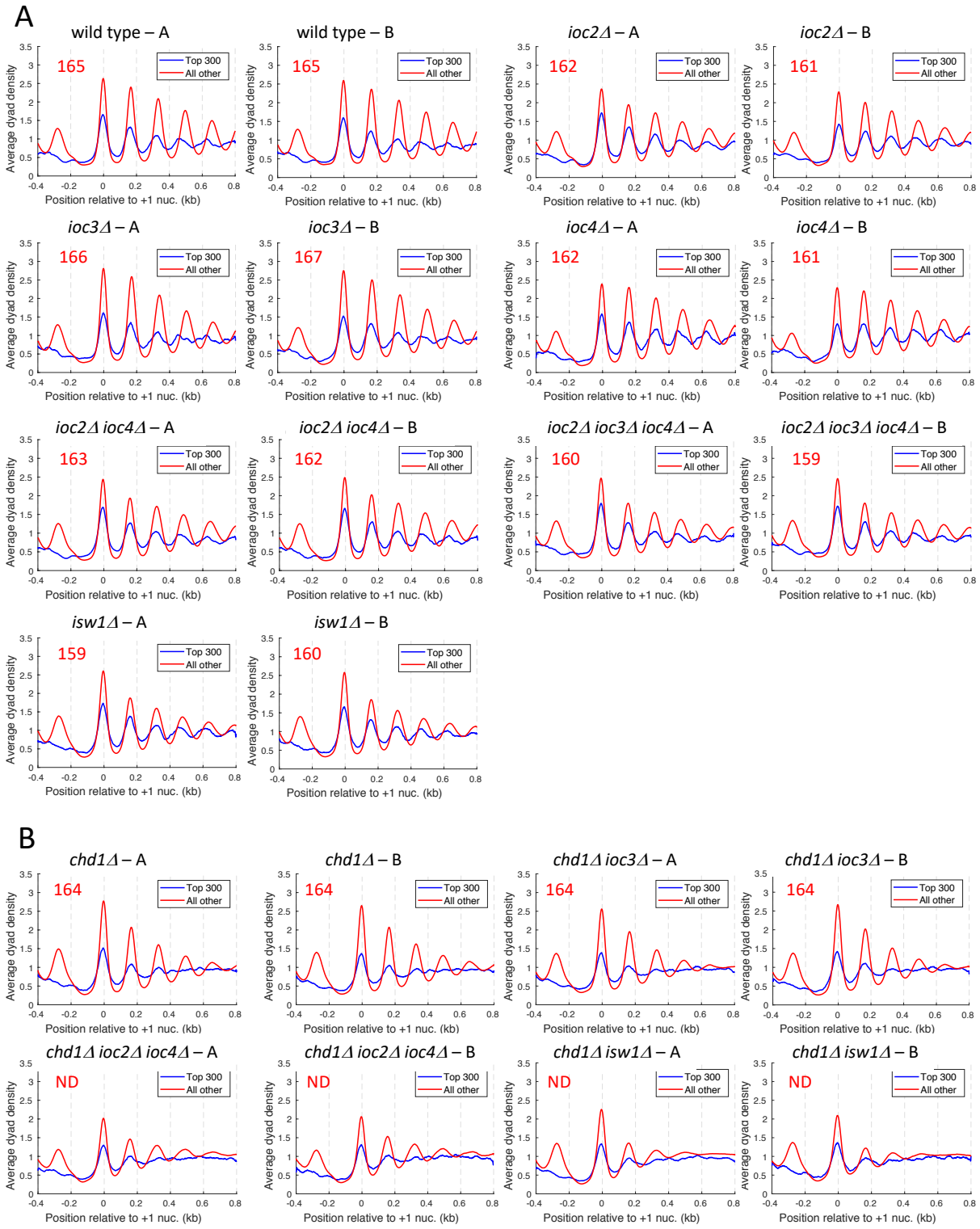

Figure S2: *continued on next page*.

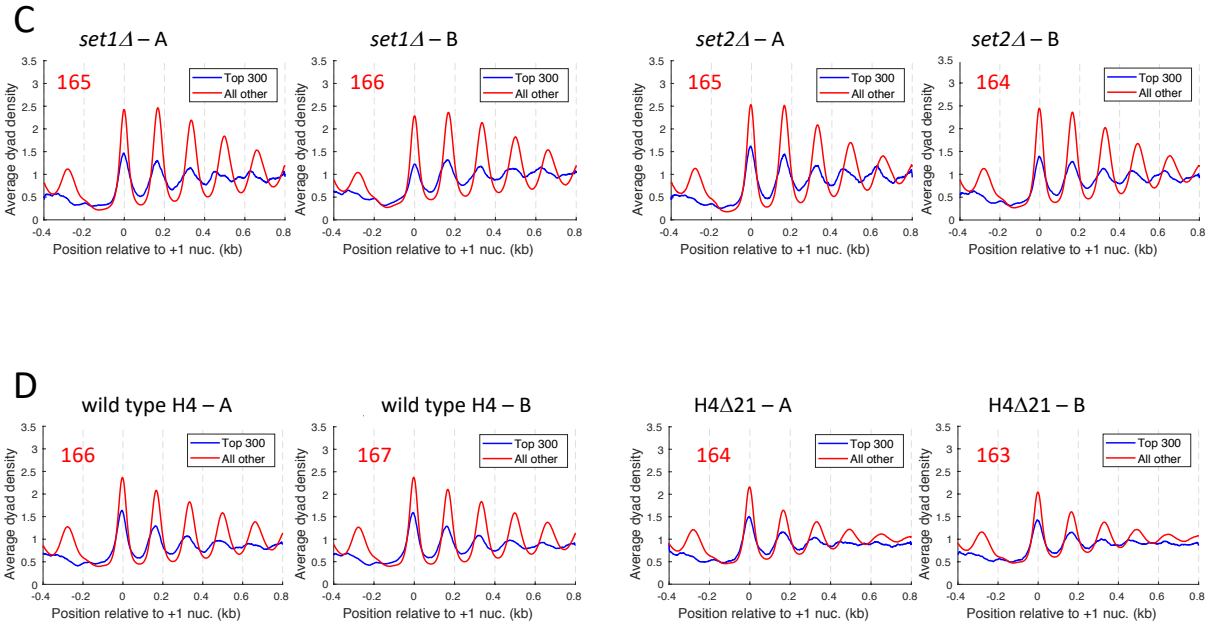

Figure S2. Chromatin organization of the top 300 most transcriptionally active genes (defined by Pol II density using ChIP-seq data for the Rpb3 subunit in wild type cells; ***Ocampo et al., 2016***). Average nucleosome dyad density plots for the 300 most active genes (blue line) compared with the remaining 5470 genes (red line). Genes were aligned on the midpoints of their +1 nucleosomes. The dyad distribution was normalized to the global average (set at 1). Two biological replicate experiments (A and B) are shown in separate panels. The average spacing in bp is shown for the top 300 active genes (blue text) and the other genes (red text), as measured by regression analysis of the first 5 nucleosome peaks, beginning with the +1 nucleosome. (**A**) Wild type (WT), *ioc2Δ*, *ioc3Δ ioc4Δ*, *ioc2Δ*, *ioc2Δ ioc4Δ*, *ioc2Δ ioc3Δ ioc4Δ* and *isw1Δ*. (**B**) *chd1Δ*, *chd1Δ ioc3Δ*, *chd1Δ ioc2Δ ioc4Δ* and *chd1Δ isw1Δ*. (**C**) *set1Δ* and *set2Δ*. (**D**) Wild type H4 and H4Δ21.

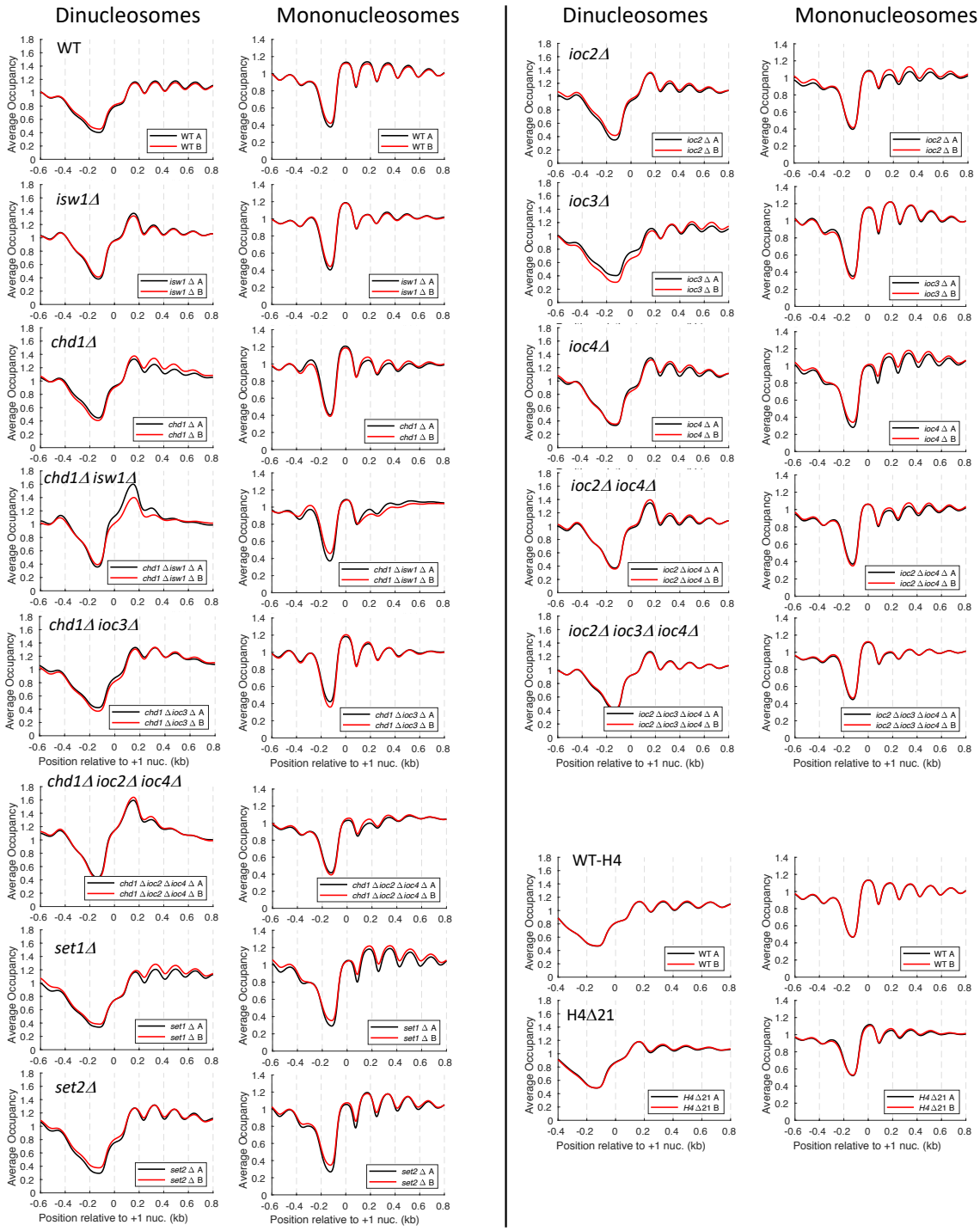

Figure S3. Mononucleosome and dinucleosome occupancy plots for all strains. Comparison of biological replicate experiments. Average nucleosome occupancy (coverage) plots for all genes. All 5770 yeast genes were aligned on the midpoint of their average +1 nucleosome position. The occupancy was normalized to the global average (set at 1) for dinucleosomes (250 - 350 bp; left panels) or mononucleosomes (120 - 180 bp; right panels). Note different y-axis scales are used in the dinucleosome and mononucleosome plots. Replicate A (black line); replicate B (red line).

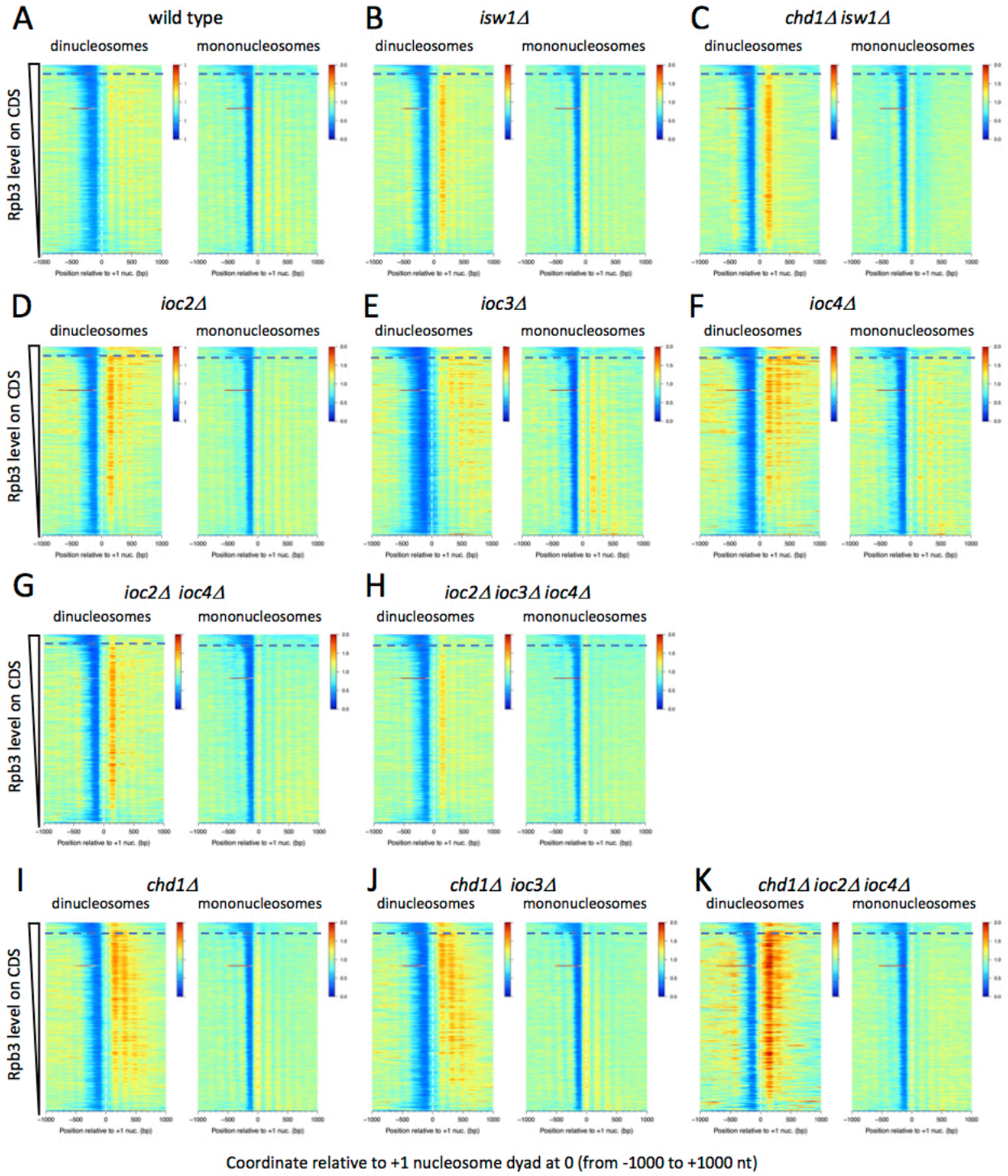

Figure S4: *continued on next page*.

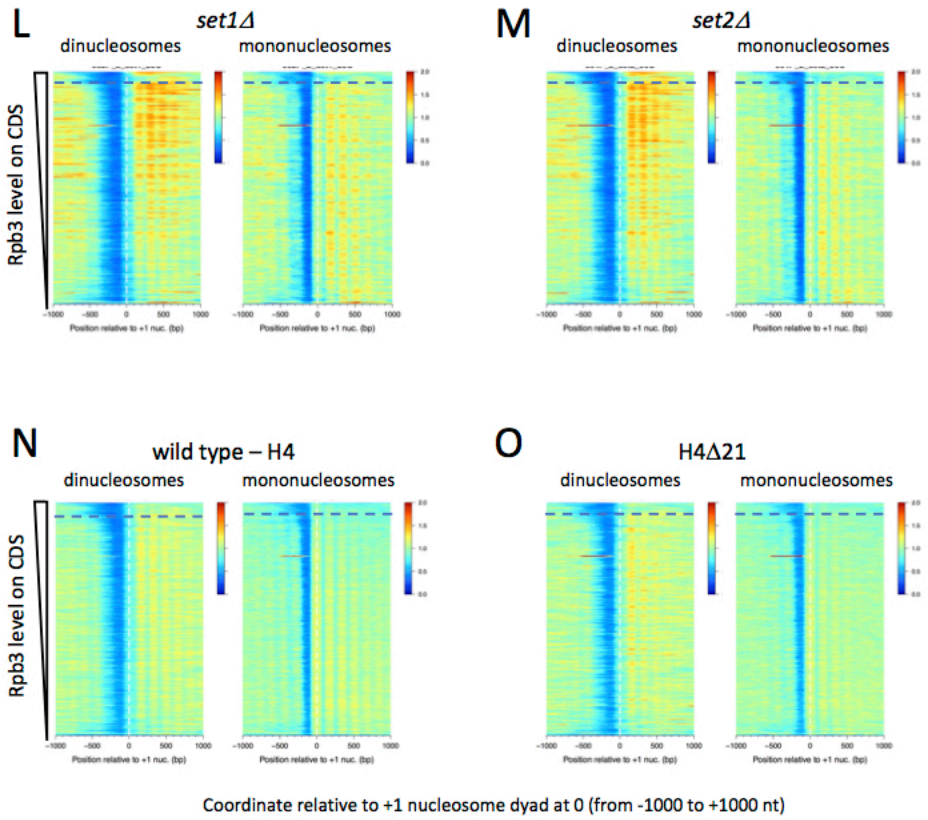

Figure S4. Dinucleosome formation correlates with RNA polymerase II levels, except for the most highly transcribed genes. Heat map analysis of nucleosome occupancy (coverage) for all genes aligned on the midpoint of their average +1 nucleosome position and sorted by Pol II density on the coding region (CDS), using ChIP-seq data for the Rpb3 subunit (***Ocampo et al., 2016***). Data for replicate B are shown (see ***Figures 4, 5 and 6*** for replicate A). The dashed line separates the top 300 most active genes from the rest. The scale bar is the same for all plots, ranging from blue (low nucleosome occupancy) to red (high occupancy). (**A**) wild type, (**B**) *isw1Δ*, (**C**) *chd1Δ isw1Δ*, (**D**) *ioc2Δ*, (**E**) *ioc3Δ*, (**F**) *ioc4Δ*, (**G**) *ioc2Δ ioc4Δ*, (**H**) *ioc2Δ ioc3Δ ioc4Δ*, (**I**) *chd1Δ*, (**J**) *chd1Δ ioc3Δ*, (**K**) *chd1Δ ioc2Δ ioc4Δ*, (**L**) *set1Δ*, (**M**) *set2Δ*, (**N**) wild type-H4 and (**O**) H4Δ21.

Supplementary Tables

Table S1. Primers used in this study.

1770 (H4Δ21) ACTGTTCCGAGCGCTTCT
1771 (H4Δ21) [5'-phosphate]-CATATTTTACTATATTATATTTGTTGCTTG
1773 (H4Δ21) CGAATTGGAGCTCGGTAC
1812 (H4Δ21) [5'-phosphate]-CTAAGAGATAACATCCAAGGTATTAC
1914 (set2) AAAACTGCATAGTCGTGCTGTCAAACCTTTCTCCTTTCCTGGTTGTTGTTTTACGTGATCCGGATCCCCGGGTTAATTAA
1915 (set2) ACAAGACTTCCTTTGGGACAGAAAACGTGAAACAAGCCCCAAATATGCATGTCTGGTTAAGAATTCGAGCTCGTTTAAAC
1916 (set2) TCGCAGTAATAAGGACAGTATCCG
1917 (set2) GCAGTTAACATGTAAATTTCCCGAT
1918 (ioc3) TTCACAAGATAACTACGACCCTCC
1919 (ioc3) GATAACAGTATGCCGTTTTACCAC
1922 (ioc4) TTCTGGTTTGTTTCTTTGCCTCA
1923 (ioc4) CATATACGGTGTTAAGATGATGACA
1926 (set1) AGGTTCATTAAATGCTTGGCTT
1927 (set1) TTCTGGAGCGTATCTAATTGCTTG
1961 (ioc2)
GTGAATCAGCGATCGATGAGAACGAAGAGAACTAGGAGTACAAGAAATGTAGGAGCGAGCTTGTTCTTGATTTGTGCCCCGTA
1962 (ioc2) ATGAAGAACCAGTTGATATATATTTTACTATATACTTTTGCTGTGTATTTCTATATGAGGTGGTTTCAGGGTCCATAAAGC
1965 (ioc2) AGTGAAATACTTAACAATTGAGCTG
1966 (ioc2) GCTCCTACATTTCTTGTACTCCT

Table S2. Yeast strains used in this study. All are W303 *RAD5* background (***Zhao et al., 1998***).

Strain	***Genotype***	***Source***
YDC111	*MATa ade2-1 can1-100 leu2-3,112 trp1-1 ura3-1*	Kim 2006
YTT186	*MATa ade2-1 can1-100 his3-11,15 leu2-3,112 trp1-1 ura3-1 isw1Δ::ADE2*	Tsukiyama 1999
YTT196	*MATα ade2-1 can1-100 his3-11,15 leu2-3,112 trp1-1 ura3-1 isw2Δ::LEU2*	Tsukiyama 1999
YTT645	*MATa ade2-1 can1-100 his3-11,15 leu2-3,112 trp1-1 ura3-1 ioc3Δ::KanMX*	Tsukiyama Lab (unpub.)
YTT827	*MATa ade2-1 can1-100 his3-11,15 leu2-3,112 trp1-1 ura3-1 ioc4Δ::HPH1*	Tsukiyama Lab (unpub.)
YTT1986	*MATα ade2-1 can1-100 his3-11,15 leu2-3,112 trp1-1 ura3-1 set1Δ::NAT1*	Tsukiyama Lab (unpub.)
YJO482	*MATa ade2-1 can1-100 his3-11,15 leu2-3,112 trp1-1 ura3-1 chd1Δ::HIS3MX6*	Ocampo 2016
YJO484	*MATa ade2-1 can1-100 his3-11,15 leu2-3,112 trp1-1 ura3-1 isw1Δ::ADE2 chd1Δ::HIS3MX6*	Ocampo 2016
YJO486	*MATa ade2-1 can1-100 his3-11,15 leu2-3,112 trp1-1 ura3-1 isw2Δ::LEU2 chd1Δ::HIS3MX6*	Ocampo 2016
YJO487	*MATα ade2-1 can1-100 his3-11,15 leu2-3,112 trp1-1 ura3-1 isw2Δ::LEU2 chd1Δ::HIS3MX6*	This study
YJO505	*MATa/α ade2-1/ade2-1 can1-100/can1-100 his3-11,15/his3-11,15 leu2-3,112/leu2-3,112 trp1-1/trp1-1 ura3-1/ura3-1 ISW1/isw1Δ::ADE2 ISW2/isw2Δ::LEU2 RSC8/GALp-RSC8::KanMX CHD1/chd1Δ::HIS3MX6*	Ocampo 2016
YPE600	*MATa/α ade2-1/ade2-1 can1-100/can1-100 his3-11,15/HIS3 leu2-3,112/leu2-3,112 trp1-1/ trp1-1 ura3-1/ura3-1 isw2Δ::LEU2*	This study

YPE606	*MATa ade2-1 can1-100 leu2-3,112 trp1-1 ura3-1 ioc3Δ::KanMX*	This study
YPE607	*MATα ade2-1 can1-100 leu2-3,112 trp1-1 ura3-1 ioc3Δ::KanMX*	This study
YPE608	*MATa ade2-1 can1-100 leu2-3,112 trp1-1 ura3-1 ioc4Δ::HPH1*	This study
YPE636	*MATa ade2-1 can1-100 leu2-3,112 trp1-1 ura3-1 ioc2Δ::URA3*	This study
YPE654	*MATa ade2-1 can1-100 leu2-3,112 trp1-1 ura3-1 ioc2Δ::URA3 ioc3Δ::KanMX*	This study
YPE655	*MATa ade2-1 can1-100 leu2-3,112 trp1-1 ura3-1 ioc2Δ::URA3 ioc4Δ::HPH1*	This study
YPE657	*MATa ade2-1 can1-100 leu2-3,112 trp1-1 ura3-1 ioc2Δ::URA3 ioc3Δ::KanMX ioc4Δ::HPH1*	This study
YPE712	*MATa ade2-1 can1-100 his3-11,15 leu2-3,112 trp1-1 ura3-1 chd1Δ::HIS3MX6 ioc3Δ::KanMX6*	This study
YPE715	*MATa ade2-1 can1-100 his3-11,15 leu2-3,112 trp1-1 ura3-1 chd1Δ::HIS3MX6 ioc2Δ::URA3 ioc4Δ::HPH1*	This study
YPE602	*MATa ade2-1 can1-100 leu2-3,112 trp1-1 ura3-1 set1Δ::NAT1*	This study
YPE604	*MATa ade2-1 can1-100 leu2-3,112 trp1-1 ura3-1 set2Δ::TRP1*	This study
ROY1281	*MATα lys2 trp1 his3 leu2 ura3 hhf1-hht1Δ::LEU2 hhf2-hht2Δ::HIS3 pCC67*	Dhillon 2000
YDC507	*MATα lys2 trp1 his3 leu2 ura3 hhf1-hht1Δ::LEU2 hhf2-hht2Δ::HIS3 p730*	This study
YDC101	*MATα lys2 trp1 his3 leu2 ura3 hhf1-hht1Δ::LEU2 hhf2-hht2Δ::HIS3 p368*	This study

Supplementary References

Dhillon, N., Kamakaka, R.T., 2000. A histone variant, Htz1p, and a Sir1p-like protein, Esc2p, mediate silencing at HMR. Mol. Cell 6, 769–780. doi:10.1016/s1097-2765(00)00076-9

Kim, Y., McLaughlin, N., Lindstrom, K., Tsukiyama, T., Clark, D.J., 2006. Activation of Saccharomyces cerevisiae HIS3 results in Gcn4p-dependent, SWI/SNF-dependent mobilization of nucleosomes over the entire gene. Mol. Cell. Biol. 26, 8607–8622. doi:10.1128/MCB.00678-06

Ocampo, J., Chereji, R.V., Eriksson, P.R., Clark, D.J., 2016. The ISW1 and CHD1 ATP-dependent chromatin remodelers compete to set nucleosome spacing in vivo. Nucleic Acids Res. 44, 4625–4635. doi:10.1093/nar/gkw068

Tsukiyama, T., Palmer, J., Landel, C.C., Shiloach, J., Wu, C., 1999. Characterization of the imitation switch subfamily of ATP-dependent chromatin-remodeling factors in Saccharomyces cerevisiae. Genes Dev. 13, 686–697. doi:10.1101/gad.13.6.686

Yen, K., Vinayachandran, V., Batta, K., Koerber, R.T., Pugh, B.F., 2012. Genome-wide nucleosome specificity and directionality of chromatin remodelers. Cell 149, 1461–1473. doi:10.1016/j.cell.2012.04.036

Zhao, X., Muller, E.G., Rothstein, R., 1998. A suppressor of two essential checkpoint genes identifies a novel protein that negatively affects dNTP pools. Mol. Cell 2, 329–340. doi:10.1016/s1097-2765(00)80277-4